IAVCEI Commission on Volcano Geology
3rd International Workshop, Etna-Aeolian Islands
July 3-10, 2016

Abstract Book

"Geological fieldwork in volcanic areas:

mapping techiques and applications"

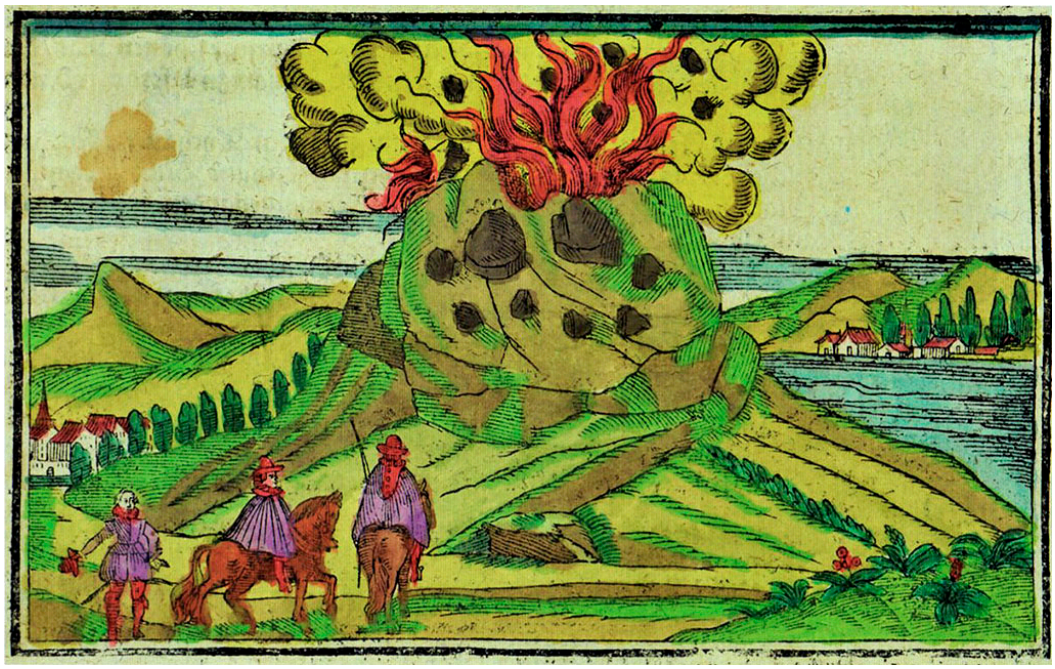

Münser 1628

Organising Committee

S. Branca, E. De Ben (INGV – OE, Italy)

G. Groppelli (CNR – IDPA, Italy)

F. Lucchi (BIGEA, University of Bologna, Italy)

R. Sulpizio (DSTG, University of Bari, Italy)

Scientific Committee

A. Brum de Silveira (University of Lisbon, Portugal)

L. Capra (Centro de Juriquilla, UNAM, Mexico)

R. Cas (Monash University, Australia)

M. Coltelli (INGV-OE, Italy)

N. Geshi (Geological Survey of Japan)

G. Giordano (University of Roma-3, Italy)

R. Isaia (INGV-OV, Italy)

J. Linday (The University of Auckland, New Zeland)

J.L. Macias (Centro de Michioacan, UNAM, Mexico)

J. Martì (ICTJA, CSIC, Barcelona, Spain)

K. Nemeth (Massey University, New Zeland)

C. Principe (CNR-IGG, Italy)

Editing abstract book

S. Massaro (DSTG, University of Bari, Italy)

Geological mapping and stratigraphy in volcanic areas on tropical environments: The case of Costa Rica, Central America

Guillermo E. Alvarado

Red Sismológica Nacional (UCR-ICR), Área de Amenazas y Auscultación Sísmica y Volcánica, Instituto Costarricense de Electricidad, Apdo. 10032-1000, COSTA RICA, (galvaradoi@ice.go.cr).

The volcano stratigraphy in Costa Rica since the end of 1950s has followed the traditional methods of oil and sedimentary stratigraphy based on the International Stratigraphic guide. However, these classical rules are no fully applied to Quaternary Geology on volcanic chains, as well as on their ignimbritic and epivolcanic aprons. On the other hand, in cases where those methods could be applied, hundreds of formal units (Formations, Members, etc.) would be generated, which are unpractical for geologist that works in other research fields (ground water supplied, applied geology, etc.). In Costa Rica, unconformities (period of quiescence, erosional phases, volcano-tectonic events) and their geographic extension have been used in the Mesozoic and Cenozoic volcanic areas. In volcanic environments we distinguish between two principal unconformities following traditional textbook of Stratigraphy and Structural geology: a) Local, parallel or erosive unconformity, when two units are separated by an erosive interval without tectonic deformation (orogeny), b) Angular unconformity, representing long erosive period in which the older strata dip at a different angle (generally steeper) than the younger strata, and is tectonically tilted or folded, and not parallel to those above. The first type is the most abundant in Quaternary setting, whereas the second type usually is older than active volcanoes, and indicates regional deformation.

Lateral collapses, include large failures mostly involving the top of the volcanic edifice (sector collapse type), and failure of the volcano summit (flank collapse type), are almost omnipresent in every large stratovolcano/shield due the humid conditions (pluvial precipitation of 4 – 8 m/year), volcanic clay soils, and hydrothermal alteration, with frequent intermediate magnitude earthquakes (one local and shallow event of Mw 5.5 – 6.5 every ~ 10 years). Although local sector collapse events defined local unconformities that are very important for local maps, in the case of Costa Rica they are no used for global volcano-stratigraphy along the volcanic chain.

Since 1980s, more extensive volcanological studies and field mapping began to define a better volcanic stratigraphy, with a resolution higher than “Undifferentiated Quaternary volcanic rocks”. For Costa Rica Quaternary Volcanic Front, we used the regional geomorphological patters to define different evolutions of the volcanoes (stratovolcanoes and andesite shield volcanoes), and correlate along the volcanic chain, by using primary to third-order unconformities/discontinuities-bounded units, which represent construction and destruction stages. The shifting of eruptive centers in a relative short time (≤ 50 ka) can be detected by geological and geomorphological criterions, and allows the establishment of subunits, although is not adhering to standard stratigraphy due their

lithological similarity and presence of third-order unconformity. The units have been named according to the nearest place names. These studies were in close collaboration between field geologist and geochronologist together with geochemistry and other laboratory analyses, in order to generate a qualified, practical and logic geovolcanological maps. Several absolute age determinations include Ar/Ar, K/Ar, U/Th and ^{14}C methods.

In this framework, Costa Rica eruptive history encompasses volcanic rocks represented on the maps of each volcano by informal units with similar patterns in the lithology, petrography, geomorphology, age range, and genesis, most of them separated as unconformity-bounded units (U.B.U.). Thus, in general, the Quaternary volcanoes of Costa Rica grew during the last 1 Ma with 3 major episodes (Systems) of cone/shield building products at 1.61 – 0.85 Ma (Proto-Cordillera), 0.74 – 0.25 (Pre-Cordillera) and < 0.25 Ma (Neo-Cordillera) separated by the 0.1 – 0.3 Ma intervals of dormancy (erosion) and/or explosive silicic volcanism. Explosive silicic eruptions are an integral part of the evolution of these composite volcanoes, with ignimbrite-forming eruptions at 0.92, 0.52, 0.49 – 0.44, and 0.325 Ma. Tephrocronology and paleosol correlation are very useful for the Late Pleistocene/Holocene record, allowing the correlation and establishment of the relative position of the main explosive and sedimentary events, including lava flows, volcanic debris avalanches, lahars, pyroclastic density currents, and also for paleoseismological and archaeological studies.

The plinian fallout tephras are useful to correlated volcanic events between neighbor volcanoes using as marker layers. The volcano maps itself and its units are useful for local studies as hydrogeology, geothermic exploration, soil geology, neotectonic, construction materials exploitation, and hazards studies. In Costa Rica, the term lithesome for the definition of eruptive centers was applied with similar philosophy, although the terminology was still not used. The reason is because the Stratigraphic code was first and it has a strong tradition between the Central American geologists. We did not differentiate or called formal lithostratigraphic units (Formations, Members) on volcanoes. We do not want to created dozens Formations in each volcano, and therefore, hundred along the Costa Rica volcanic chain, and thousands along the Central America volcanic chain, because the formal lithostratigraphic units (Super Group, Group, Formation, and Member) do not have political boundaries. In addition, in Central America there are several volcanic fronts since Paleocene which can be separated by angular unconformities (Supersystems or Super Group). Therefore, from our experience, we propose that local units should be integrated into regional major lithostragraphic units, in order to be in agreement to the traditional stratigraphy, and the local Stratigraphic Code, which are commonly used for the majority of the Central American geologist.

The final idea is that the maps on volcanic areas (active or extinct volcanic ranges), at different scales, and under tropical environments), in several cases with poor outcrops and difficult accessibility, could be useful for different professionals (geologist, geographer, biologist, engineering, etc.), but also to foment a mutual understanding between geologists from neighbor countries, allowing regional correlation.

Mapping geology for the exploration of remote geothermal fields: The Tocomar Geothermal System case study (Puna plateau, Argentina)

W. Baez[1], G. Groppelli[2], G. Giordano[3], F. Ahumada[1], L. Aldega[4], R. Becchio[1], S. Bigi[4], C. Caricchi[3], A. Chiodi[1], S. Corrado[3], A.A. De Benedetti[3], A. Favetto[5], R. Filipovich[1], A. Fusari[6], C. Invernizzi[6], R. Maffucci[3], G. Norini[2], A. Pinton[3], C. Pomposiello[5], F. Tassi[7], S. Taviani[3], J. Viramonte[1]

[1] Universidad Nacional de Salta, Salta, Argentina; [2] CNR IDPA, Milan, Italy; [3] Università Roma Tre, Roma, Italy; [4] Università La Sapienza, Roma, Italy; [5] CONICET, Buenos Aires, Argentina; [6] Università di Camerino, Camerino, Italy; [7] Università di Firenze, Firenze, Italy; (gianluca.groppelli@cnr.it).

The reconstruction of the stratigraphical and structural framework of geothermal areas is fundamental for understanding the relationships between cap rocks, reservoir and circulation of geothermal fluids and for planning the exploitation of geothermal fields. The Tocomar geothermal volcanic area (Puna plateau, Central Andes, NW Argentina) is located in an area characterised by numerous volcanic edifices active from Miocene to Holocene (e.g. from Aguas Calientes Caldera to Tuzgle volcano) and is crossed by the active NW–SE trans-Andean tectonic lineament known as the Calama–Olacapato–Toro (COT) fault system (Giordano et al., 2013; Norini et al., 2013).

The stratigraphy of the Tocomar geothermal volcanic area allows recognising pre-Tocomar basin units and the volcano-sedimentary basin fill. The oldest basement unit outcropping in the Tocomar area is the Faja Eruptiva Fm. formed by Ordovician metagranites and minor mafic intrusive rocks that intrude the Pre-Paleozoic metasedimentary Puncoviscana Fm. Above the Palaeozoic basement rocks, the oldest rocks preserved are the Cretaceous–Oligocene syn-rift and post-rift sediments (Salta Group) that were deposited along narrow grabens in rapid subsidence (Salfity and Monaldi, 2006). They are made of poorly sorted conglomerates and breccias, and fluvial–lacustrine sandstones, with a typical red-purple colour (syn-rift Pirgua Subgroup). The youngest pre-Tocomar basin unit is represented by extensive dacitic crystal rich ignimbrite sheets sourced between 17 and 10 Ma from the Aguas Calientes Caldera (Petrinovic et al. 2010). The ignimbrites are extensively lithified with diffuse vapour phase crystallisation of the matrix.

The Tocomar basin fill starts with a 12 m thick (minimum thickness) tabular and internally stratified medium to coarse sandstone, inter-bedded with thin mudstone levels, related to distal alluvial fans sedimentation (Red Sandstone unit). Coarse alluvial/fluvial sediments (Green Conglomerate unit) with a minimum thickness of 40 m filled the basin after a tectonic?-erosional phase. A coeval mafic phreatomagmatic activity is evidenced by pyroclastic surge deposits inter-bedded with the Green Conglomerate unit. Also, the presence of ~ 5m thick travertine at the top of the Green conglomerate unit points out the onset of the geothermal activity into the Tocomar basin. The Tocomar 1 pyroclastic sequence (fall/surge/flow deposits) related to a rhyoltic phreato-plinian eruption (0.55 Ma; Petrinovic and Colombo, 2006; Petrinovic et al., 2006) covers by a mild angular unconformity the Green Conlgomerate unit. This felsic volcanism was followed by other two rhyolitic

phreatomagmatic eruptions associated with different vents that formed the pyroclastic sequences (dominantly surge deposits) of Tocomar 2 and Tocomar 3. Finally, thin alluvial, fluvial and aeolian recent deposits cover largely the Tocomar basin.

References

Giordano G., Pinton A., Cianfarra P., Baez W., Chiodi A., Viramonte J., Norini G., Groppelli G. (2013). Structural control on geothermal circulation in the Cerro Tuzgle–Tocomar geothermal volcanic area (Puna plateau, Argentina). J. Volcanol. Geotherm. Res. 249, 77–94.

Norini G., Baez W., Becchio R., Viramonte J., Giordano G., Arnosio M., Pinton A., Groppelli G. (2013). The Calama–Olacapato–El Toro Fault System in the Puna Plateau, Central Andes: geodynamic implications and stratovolcanoes emplacement. Tectonophysics 608, 1280–1297.

Petrinovic I.A., Martí J., Aguirre-Díaz G.J., Guzmán S., Geyer A., Salado Paz N. (2010). The Cerro Águas Calientes caldera,NWArgentina: an example of a tectonically controlled, polygenetic collapse caldera, and its regional significance. J. Volcanol. Geotherm. Res. 194, 15–26.

Salfity J.A. and Monaldi C.R.(2006). Hoja Geológica 2566-IV: Metán (1:250,000). Programa Nacional de Cartas Geológicas de la República Argentina, boletin, 319, Buenos Aires, 80 pp.

Geological constrain for the volcanic hazard assessment on Lanzarote, in the frame of the VETOOLS Project

Laura Becerril, Stefania Bartolini, Joan Martí

Group of volcanology, (SIMGEO-UB) CSIC, Institute of Earth Sciences Jaume Almera, Barcelona, Spain.

Forecasting future eruptions has become one of the priority lines in modern volcanology. This task relies mostly on volcano monitoring data and mathematical modelling, and focuses mostly on when the next eruption may occur. However, equally important should be to determine the exact position of new vent(s) and how this next eruption may be, two aspects that should rely mostly on the past geological record of the volcanic system. Therefore, eruption forecasting should also be based on comprehensive and accurate geological studies of active volcanic areas. In particular, eruptions in monogenetic volcanic fields are sometimes difficult to forecast because firstly, attention has been mainly focused on central volcanoes where more research on volcanic hazard assessment has been done, but also due to the lack of knowledge on the precursory activity of this volcanism. Keeping in mind also that monogenetic volcanism is the most common and frequent type of volcanism on Earth, it is important to study this kind of volcanic activity, characterising its volcano-structural controls, its most common volcano-types, deposits and forms, the petrology and size of the eruptions and their eruptive styles, the eruption frequency, as well as the most expected hazards, in order to know how future eruptions might be on these fields.

Here, we present a volcano-structural analysis and the characterisation of past eruptive activity that have allowed us to obtain the input parameters required for conducting volcanic hazard assessment in Lanzarote (Canary Islands, Spain). The obtained results are: (1) the vocano-structural configuration of Lanzarote that constitutes the basis for subsequent susceptibility studies; and (2) the main input parameters for the simulation models with which we have performed different volcanic scenarios such as lava flows, ash-fall and pyroclastic density currents (PDCs). Both, volcano-structural data and volcanological parameters have been gathered from the geological record, mainly from recent and historical eruptions on the island, and previous published studies.

From the volcano-structural study we have obtained different datasets that correspond to vents and eruptive fissures, both onshore and offshore the island, and faults, also taking into account the current stress field of the area. Volcano-structural datasets were divided according to the age of the structures. Thus we obtained (23,1) Miocene-Pliocene, (419,69) Pleistocene and (171,25) Holocene onshore vents, and eruptive fissures respectively. The number of eruptive vents offshore reaches 102 and 9 eruptive fissures. Only 6 faults have been identified on the island. The majority of the linear structures (eruptive fissures and faults) follow the NE-SW direction and they are from less than 1 km to 15 km length. All these datasets were converted into probability density functions

(PDFs) and weighed through an Expert Judgement Elicitation in order to provide initial indicative probability distributions associated with each PDF. From the eruptive characterisation we set that mafic monogenetic eruptions with clear Strombolian character represent the most likely eruption types in the near future on the island. Parameters to simulate lava flows, ashfall and PDCs were derived from the most recent eruptions on the island (historical eruptions that took place in the last 600 yr: 1730-36 and 1824 eruptions). Lava flows reach minimum lengths of 1.5 km, 5-7 km as average and maximum lengths of 25 km, being normally up to 10 m thick. Thus, Timanfaya eruption (1730-36) would represent the worst scenario (in terms of size, long duration, magnitude and volume emitted), where the volume considered was 4 km^3 with eruptive columns that reached probably around 5 km high. While the 1824 eruption represents the most common eruption on the island, being the parameters derived from it, 0.02 km^3 emitted volume with 3 km of eruptive column. In both eruptions grans size distribution was obtained from each representative deposit. Parameters to simulate PDCs were extracted from hydromagmatic eruptions or strombolian ones with phreatomagmatic phases, being the maximum observed run-out distances of PDCs of 3 km.

All these results show that likely future volcanic activity in Lanzarote can be understood and predicted via the analysis of past eruptive behaviour and the study of the geological record. This work has been developed in the frame of the VeTOOLS project (EC ECHO project; SI.2.695524; 2015-2016).

Tephra in marine sediment cores offshore southeast Iceland: A 68,000 year volcanic record

Christina Bonanati, Heidi Wehrmann, Maxim Portnyagin, Kaj Hoernle

RD4 Dynamics of the Ocean Floor, Magmatic and Hydrothermal Systems. GEOMAR Helmholtz Centre for Ocean Research Kiel, Wischhofstr. 1-3, 24148 Kiel, Germany, (cbonanati@geomar.de).

Icelandic explosive volcanic eruptions have far-reaching impacts. Twenty eruptions per century have been recorded in historical time (Larsen and Eiríksson, 2008; Thordarson and Höskuldsson, 2008). Wide-spread tephra has been found up to Northern Continental Europe and Greenland (e.g. Grönvold et al., 1995; Dugmore, 1996; Lacasse et al., 1998; Jennings et al., 2000; Larsen et al., 2000; Wastegård et al., 2001; van den Bogaard and Schmincke, 2002; Pilcher et al., 2005; Davies et al., 2014). On Iceland, erosion and ice cover limit the preservation and accessibility of volcanic deposits, limiting knowledge about Icelandic volcanic activity in pre-Holocene periods. We use the marine sedimentary archive offshore southeast Iceland which preserves information about the depositional fans at medial distance from the volcanic source. From this geologic record we infer eruption frequencies and geochemical characteristics of the volcanic systems, thus contributing to Icelandic volcanic hazard assessment and supporting the stratigraphic framework used for palaeoceanographic reconstructions. Here we report the analysis of four sediment gravity cores obtained during RV Poseidon Cruise 457, at distances of 60 to 180 km southeast of Iceland (Fig.1). Cores of ~5 to 10 m lengths were recovered; two east of eastern Katla Ridge at the southern shelf-slope at 1300 m water depths, and two southwest of Iceland-Faroe Ridge at 1610 and 755 m water depths. We identified potential tephra layers by visual inspection and color-scans and analyzed volcanic glass shards for their major element composition using an electron microprobe. The deposits are assigned to their eruptive source by geochemical fingerprinting (Fig.2) which is unique for most Icelandic volcanic systems (Jakobsson, 1979). The tephras are geochemically correlated with previously identified deposits in European lakes and bogs, marine cores, Greenland Ice-cores and from onshore Iceland. The inter-core correlation is supported by color-scans, of which the *b-values are tied in with the $\delta^{18}O$ Greenland Ice-core record, together with prominent tephra layers, providing the age model. The record reaches back to the Late Pleistocene (~68 ka BP). We identified 25 primary and nearly as many compositionally heterogeneous tephra layers, mostly basaltic. The deposits are predominantly derived from the volcanic systems Grímsvötn-Lakagígar, Bárðarbunga-Veiðivötn, Katla and Hekla.

The Vedde-tephra

The ~12 ka BP (Rasmussen et al., 2006) Vedde-tephra with a unique bimodal composition erupted from Katla Volcanic System (Larsen et al., 2001). Vedde-rhyolite cryptotephra deposits have been reported between 8 and 15 ka BP (Lane et al., 2012 and references therein). At the studied sites,

tephra of this composition occurs at varying core depths including the late-Pleistocene parts (Fig.3). Unknown eruptions producing tephra of the Vedde composition are also possible. Tephra stratigraphy in the study area is not straightforward due to reworking and high amounts of volcanic background sediment. The presence of the Vedde-like deposits at varying depths in the upper, Holocene part of one core prompts to questioning undisturbed sedimentation conditions at this time.

"Faroe Marine Ash Zones" (FMAZ) II and III

FMAZ II has been described in several marine and ice cores (Rasmussen et al., 2003; Davies et al., 2008; Davies et al., 2012; Griggs et al., 2014, Völker and Haflidason, 2015). It occurs in core 905 and 909 at stratigraphic depths corresponding to 27-28 ka BP (Fig.3). The thickest layer is compositionally identical to the Fugloyarbanki tephra. This is the most voluminous deposit considered to be sourced from Kverkfjöll (Larsen and Gudmundsson, 2015) (Tephra F).

FMAZ III is represented by several layers of Grímsvötn composition in core 905 at depths corresponding to ages between 35 and 38 ka BP.

Before 43 ka BP, several layers have unique compositions differing from that of any Icelandic volcanic system recently active. Their geochemistry has most similarity with products from the central part of the active Icelandic rift zone. Unique compositions that are different from today's geochemistry occur only before 24 ka BP. This suggests that the major event, which produced the Fugloyarbanki tephra, might be associated with a change in magma generation or ascent at the central part of the active Icelandic rift zone. In the Holocene, Grímsvötn was far more active than Kverkfjöll (Larsen et al., 1998; Óladóttir et al., 2011). Both volcanic systems are equally well represented in the late Pleistocene record of our cores, suggesting that at this time the Kverkfjöll volcanic system has been more active in terms of explosive eruptions than in the Holocene.

Changes of geochemistry and frequency and thus magma extrusion (Larsen and Gudmundsson 1997) at the central part of the active Icelandic rift zone at around 24 ka BP might have had different causes. We expect phreatomagmatic eruptions throughout the whole record (Oladottir, 2007) which possibly varied in response to ice-cover. As unique tephras before 24 ka BP do not occur simultaneously with any allover climatic change, they are unlikely caused by interrelation of glacio-isostasy and changes on mantle melting and crustal stresses, as observed beneath Vatnajökull today (Pagli and Sigmundsson, 2008). However, the eruption events producing FMAZ II might have taken place in response to the Greenland Interstadials 3 and 4. Even though the influence of the mantle plume (Wolfe et al., 1997) may have varied over time, changes in local tectonics are more likely. Magma mixing through lateral dike propagation (McGarvie, 1984; Einarsson et al., 1997) might have happened when Kverkfjöll was tectonically closer connected with Grímsvötn and Bárðarbunga volcanic systems, changing geochemistry of volcanic products from this region.

A combination of these processes is likely. The 27 ka BP event could have caused an emptying of the magma chamber beneath Kverkfjöll and decreased magma extrusion at this system and change in the mechanical interaction and dike-connectivity with neighboring systems thereafter.

Our results extend the eruption record further back in time than currently inferred from terrestrial Iceland, and in more detail than far-distant records, and facilitates insight into the evolution of the magmatic systems at the central part of the active Icelandic rift zone.

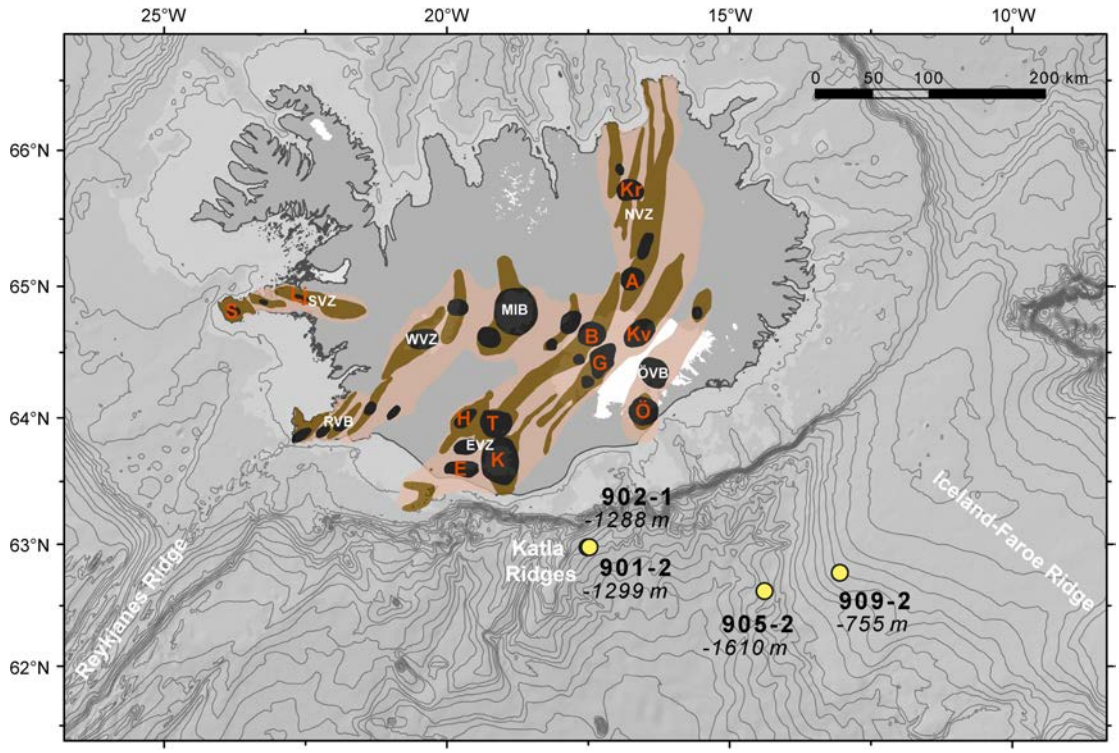

Fig.1 - *Iceland and the bathymetry of the surrounding ocean floor with sample locations and depths. Beige: volcanic zones; brown: fissure volcanoes; black: central volcanoes. Northern-Volcanic Zone (NVZ): Krafla (Kr), Askja (A), Kverkfjöll (Kv); northern part of the Eastern Volcanic Zone (EVZ): Grímsvötn-Lakagígar (G), Bárðarbunga-Veiðivötn (B). Southern part of EVZ: Hekla (H), Eyjafjallajökull (E) Torfajökull (T), Katla (K). Öræfajökull Volcanic Belt (ÖVB): Öræfajökull (Ö). Reykjanes Volcanic Belt (RVB), West Volcanic Belt (WVB), Mid Icelandic Belt (MIB). Snaefellsnes Volcanic Zone (SVZ): Sneafelsjökull (S), Ljósufjöll (Lj).*

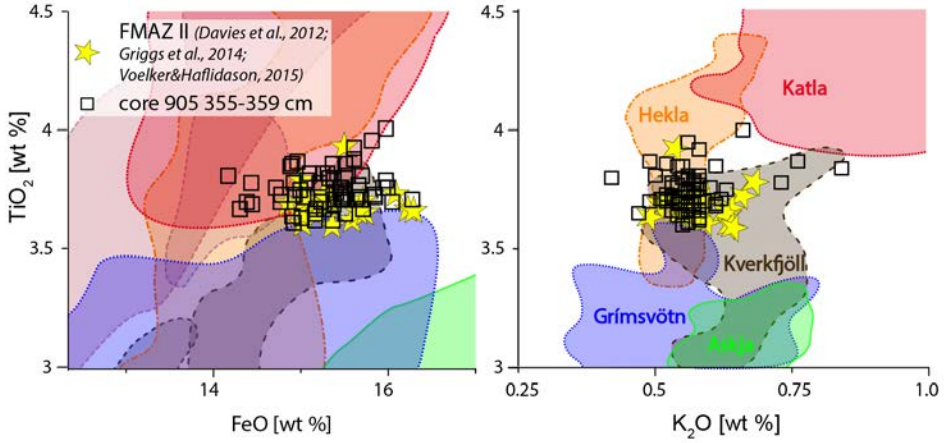

Fig. 2 - *FeO and K_2O vs. TiO_2 of glass-shards from a tephra layer in core 905 correlated with FMAZ II (Fugloyarbanki tephra, Tephra F), discriminating it from other Icelandic volcanic sources.*

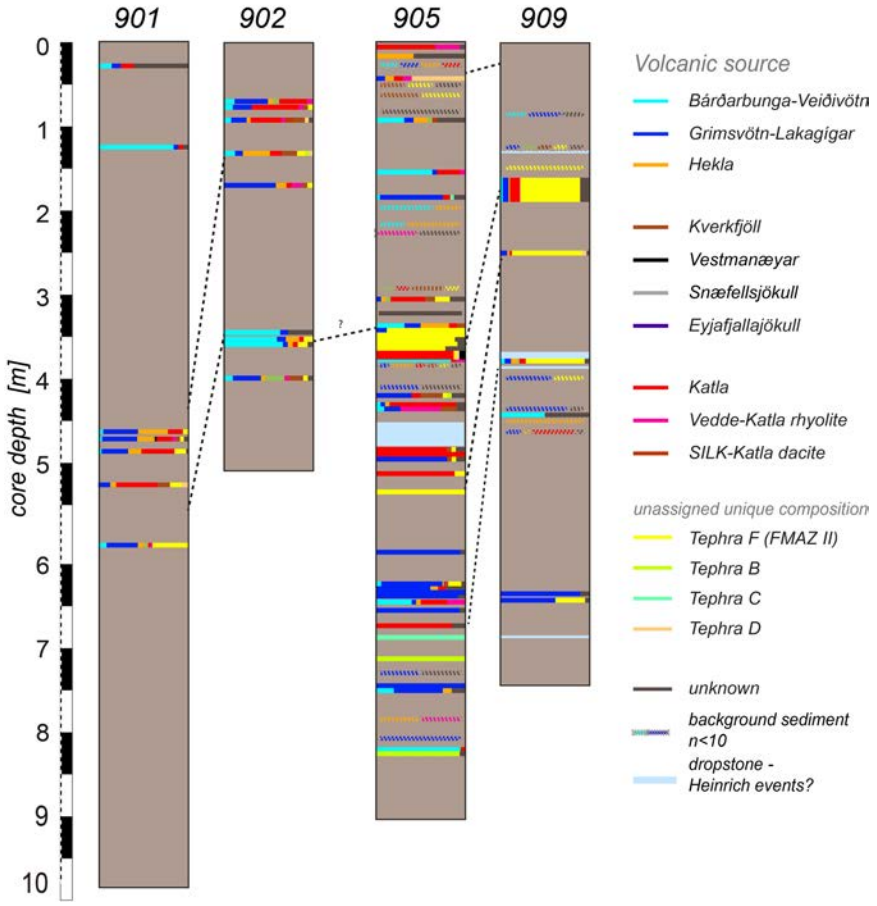

Fig. 3 - *Gravity cores from RV Poseidon cruise 457 with layers showing the distribution of tephra assigned to the Icelandic volcanic sources. Layers are 300 % vertically exaggerated.*

References

Davies S.M., Abbott P.M., Pearce N.J.G., Wastegård S., and Blockley S.P.E. (2012). ntegrating the INTIMATE records using tephrochronology: rising to the challenge: Quaternary Science Reviews 36, 11–27.

Davies S.M., Wastegård S., Rasmussen T.L., Svensson A., Johnsen S.J., Steffensen J.P., Anderesn K.K. (2008). Identification of the Fugloyarbanki tephra in the NGRIP ice core: a key tie-point for marine and ice-core sequences during the last glacial period. Journal of Quaternary Science 23, 409–414.

Dugmore A.J.(1996). Long-distance marker horizons from small-scale eruptions: British tephra deposits from the AD 1510 eruption of Hekla, Iceland. Journal of Quaternary Science 11, 511–516.

Einarsson P., Brandsdóttir B., Gudmundsson M.T., Björnsson H., Grínvold K., and Sigmundsson F. (1997). Center of the Iceland hotspot experiences volcanic unrest: Eos, Transactions American Geophysical Union 78, 35, 369–375.

Grönvold K., Johnsen S.J., Clausen H.B., Hammer C.U., Bond G., Bard E. (1995). Ash layers from Iceland in the Greenland GRIP ice core correlated with oceanic and land sediments. Earth Planetary Science Letters 35, 149–155.

Griggs A.J., Davies S.M., Abbott P.M., Rasmussen T.L., and Palmer A.P. (2014). Optimising the use of marine tephrochronology in the North Atlantic: a detailed investigation of the Faroe Marine Ash Zones II, III and IV: Quaternary Science Reviews 106, 122-139.

Jakobsson S.P.(1979). Petrology of recent basalts of the Eastern Volcanic Zone, Iceland: Acta Naturalia Islandica 28, 12, 878.

Lacasse C., Carey S., Sigurdsson H. (1998). Volcanogenic sedimentation in the Iceland Basin: influence of subaerial and subglacial eruptions. J. Volcanol. Geotherm. Res. 83, 47–73.

Lane C.S., Blockley S.P.E., Mangerud J.A.N., Smith V.C., Lohne Ø.S., Tomlinson E.L., Matthews I.P., and Lotter A.F. (2012). Was the 12.1ka Icelandic Vedde Ash one of a kind? Quaternary Science Reviews 33, 87–99.

Larsen G., Eiríksson J., Knudsen K.L., Heinemeier J. (2000). Correlation of late Holocene terrestrial and marine tephra markers, north Iceland: implications for reservoir age changes. Polar Research 21, 283–290.

Larsen G., and Eiríksson J. (2008). Late Quaternary terrestrial tephrochronology of Iceland — frequency of explosive eruptions, type and volume of tephra deposits: Journal of Quaternary Science 23, 2, 109–120.

Larsen G., Gudmundsson M.T., and Björnsson H. (1998). Eight centuries of periodic volcanism at the center of the Iceland hotspot revealed by glacier tephrostratigraphy: Geology 26, 10, 943–946.

Larsen G., Newton A.J., Dugmore A.J., and Vilmundardóttir E.G. (2001). Geochemistry, dispersal, volumes and chronology of Holocene silicic tephra layers from the Katla volcanic system, Iceland: Journal of Quaternary Science 16, 119–132.

Larsen G. and Gudmundsson M.T. (2015). The Kverkfjöll volcanic system. In: Larsen and Gudmundsson (eds.): Catalogue of Icelandic Volcanoes.

McGarvie D.W. (1984). Torfajokull: a volcano dominated by magma mixing.: Geology 12, 11, 685–688.

Óladóttir B.A., Larsen G., and Sigmarsson O. (2011). Holocene volcanic activity at Grímsvötn, Bárdarbunga and Kverkfjöll subglacial centres beneath Vatnajökull, Iceland: Bulletin of Volcanology, v. 73, no. 9, p. 1187–1208.

Pagli C., and Sigmundsson F. (2008). Will present day glacier retreat increase volcanic activity? Stress induced by recent glacier retreat and its effect on magmatism at the Vatnajökull ice cap, Iceland: Geophysical Research Letters 35, 9, 3–7.

Pilcher J.R., Bradley R., Francus, P., Anderson L. (2005). A Holocene tephra record from the Lofoten Islands, Arctic Norway. Boreas 34, 136–156.

Rasmussen S.O., Andersen K.K., Svensson A.M., Steffensen J.P., Vinther B.M., Clausen H.B., Siggaard-Andersen M.L., Johnsen S.J., Larsen L.B., Dahl-Jensen D., Bigler M., Rüthlisberger R., Fischer H., Goto-Azuma K., et al. (2006). A new Greenland ice core chronology for the last glacial termination: Journal of Geophysical Research Atmospheres 111, 6, 1–16.

Rasmussen T.L., Wastegård S., Kuijpers A., van Weering T.C.E., Heinemeier J., and Thomsen E. (2003). Stratigraphy and distribution of tephra layers in marine sediment cores from the Faeroe Islands, North Atlantic: Marine Geology, v. 199, p. 263–277.

Thordarson T., and Höskuldsson Á. (2008). Postglacial volcanism in Iceland: Jökull 58, 197–228.

Thornalley D.J.R., McCave I.N., and Elderfield H. (2011). Tephra in deglacial ocean sediments south of Iceland: Stratigraphy, geochemistry and oceanic reservoir ages: Journal of Quaternary Science 26, 2, 190–198.

van den Bogaard C., Schmincke H.-U. (2002). Linking the North Atlantic to central Europe: a high-resolution Holocene tephrochronological record from northern Germany. J. Quat. Sci. 17, 3–20.

Voelker A.H.L., and Haflidason H. (2015). Refining the Icelandic tephrachronology of the last glacial period – The deep-sea core PS2644 record from the southern Greenland Sea: Global and Planetary Change, 131, 35–62.

Wastegård S., Björck S., Grauert M., Hannon G.E. (2001). The Mjáuvøtn tephra and other Holocene tephra horizons from the Faroe Islands: a link between the Icelandic source region, the Nordic Seas, and the European continent. The Holocene 11, 101–109.

Wolfe C. J., Bjarnason I. T., VanDecar J. C., and Solomon S. C. (1997). Seismic structure of the Iceland mantle plume. Nature 385, 245-247.

A detrital investigation of enigmatic subglacial magmatic systems: Vatnajökull, SE Iceland

Tamara Carley [1], Tenley Banik [2], Alexandra Nagurney [1], Leslie Tintle [1], John Catino [3]

[1]Lafayette College (Geology and Environmental Geoscience, Easton, PA 18042, USA), (carleyt@lafayette.edu; allie.nagurney@gmail.com; tintlelr@gmail.com); [2]Illinois State University (Dept. of Geography-Geology, Normal, IL 61761, USA), (tjbanik@ilstu.edu); [3]Minerals Technologies, Inc. (Analytical Services Group, Easton, PA 18042, USA), (john.catino@mineralstech.com).

Iceland is the product of volcanism from the combined influences of a mid ocean ridge and hotspot—a unique geologic setting on modern Earth. The intersection of these two important magmatic-tectonic features is obscured by Vatnajökull, an icecap that covers ~11% of Iceland's surface area. A moderate number of central volcanoes (~5) and associated volcanic ridges and fissure swarms are known to exist beneath Vatnajökull (Fig. 1). The majority of these recognized volcanoes are notable in the annals of Icelandic geology: Öræfajökull's 1362 AD eruption was the largest explosive rhyolite eruption in historical times; Grímsvötn is the most frequently active central volcano in historical Iceland; Bárðarbunga was the most recently active (as of time of writing) in Iceland after a fissure erupted for 6 months beginning in August 2014. Many other sub-Vatnajökull volcanic systems are more obscure and enigmatic. While some sub-Vatnajökull systems have confirmed eruptive products (e.g., those listed above, Þórðarhyrna and Esjufjöll), seismic and geophysical evidence hint at additional—but largely unconfirmed and unstudied—subglacial volcanic systems.

This study uses glacially derived material (glass, lithics, and minerals) to improve understanding of the magmatic systems that lie beneath Vatnajökull. Sampling subglacial materials deposited in moraines and outwash plains is an effective method of gaining regional-scale perspective and can provide important compositional context for this critical region of Iceland. We have collected detrital samples from outlet glacier drainages around the southern and eastern perimeter of Vatnajökull (Fig. 1). Preliminary compositional analysis of mafic glass and intermediate pumice fragments via FESEM-XEDS indicates a geochemical match to sub-glacial volcanic systems known to exist in the sampled drainage basins (e.g., compositional similarity between sand from Hversfljót and compositions compiled in the GEOROC database for subglacial Grímsvötn and Þórðarhyrna). Further work to conclusively differentiate between individual volcanic centers using major, trace element, and isotopic geochemistry is ongoing. We use Excel-MELTs modeling to explore magmatic conditions for detrital materials (e.g., plausible source rock compositions and evolutionary trends; constrains on temperature and pressure of formation; influence of changing pressure regimes). Modeling based on our preliminary compositional data indicates evolutionary trends, and thus perhaps insight into pre-eruptive magmatic behavior, between compositions glass and pumice

fragments within individual drainage basins (Fig. 2). Furthermore, we demonstrate how GIS techniques can be highly effective for characterizing and interpreting: (1) physical and compositional characteristics of subaerial and subglacial aspects of drainage basins (2) compositional variation of detrital materials between discrete outlet glacier drainages; and (3) compositional similarities or variation between detrital materials and regional volcanoes. Though this detrital study lacks the precision that comes with tephra studies (which provide snapshot views of individual, point-source, subaerial eruptions), we have demonstrated that glacially derived sediments can be used to explore magmatic evolution and think about past and future behaviors of volcanic systems that are obscured from view. This approach to volcanic characterization provides a much-needed regional perspective that is especially useful for filling gaps of knowledge and revealing areas of future research in this important yet enigmatic region of Iceland. The volcanic systems beneath Vatnajökull—both the known and the unknown—are important to study because: (1) subglacial magmatic activity can lead to hazardous jökullhlaups—glacial outburst floods; (2) as observed with Eyjafjallajökull in 2010, subglacial volcanic systems are capable of hazardous and expensive phreatomagmatic explosive activity; (3) with the exception of Öraefajökull, evidence of silicic volcanism at systems beneath Vatnajökull is anomalously rare by Icelandic standards; if silicic magma is being generated at these subglacial systems, they might capable of hazardous eruptions or contribute in important ways to Icelandic crustal construction; (4) it is hypothesized that the pressure associated with glacial loading and unloading can impact the stability of shallow-crustal magma bodies, or even generate new melting. As climate continues to change and Iceland's icecaps continue to thin, there is increasing concern about the future activity of the several volcanic systems that exist beneath the ice. We (as a community of volcanologists, petrologists, and hazard planners) need to better understand past and present behavior of Subglaical systems in order to better prepare for future volcanic threats. This detrital approach is an efficient and effective way to contribute to this important task.

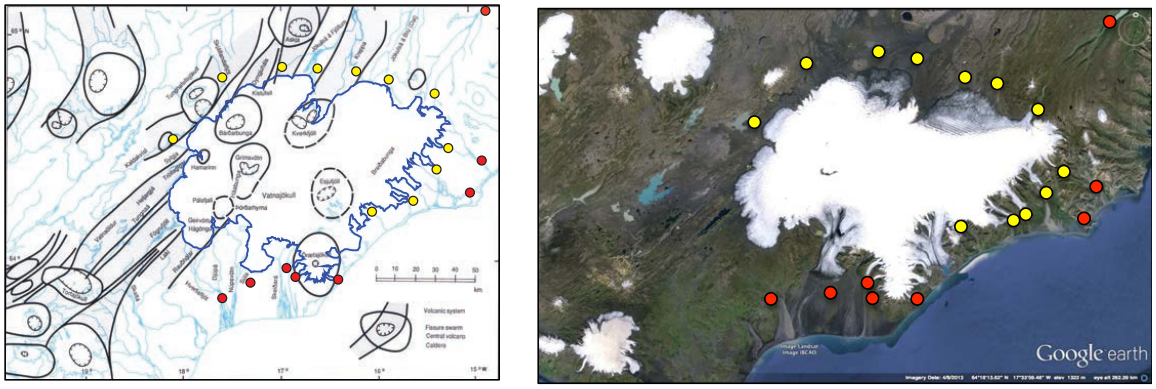

Figure 1: The map at left (modified from Björnsson and Einarsson, 1990) shows the extent of Vatnajökull (outlined in dark blue) along with central volcanoes, associated fissure swarms, and rivers and streams draining the ice cap. Samples that we have collected for this detrital investigation of subglacial volcanic systems are indicated with red circles. Samples that we plan to collect in the future are indicated with yellow circles. The same scene is depicted with modern ice extent in the Google Earth image on the right.

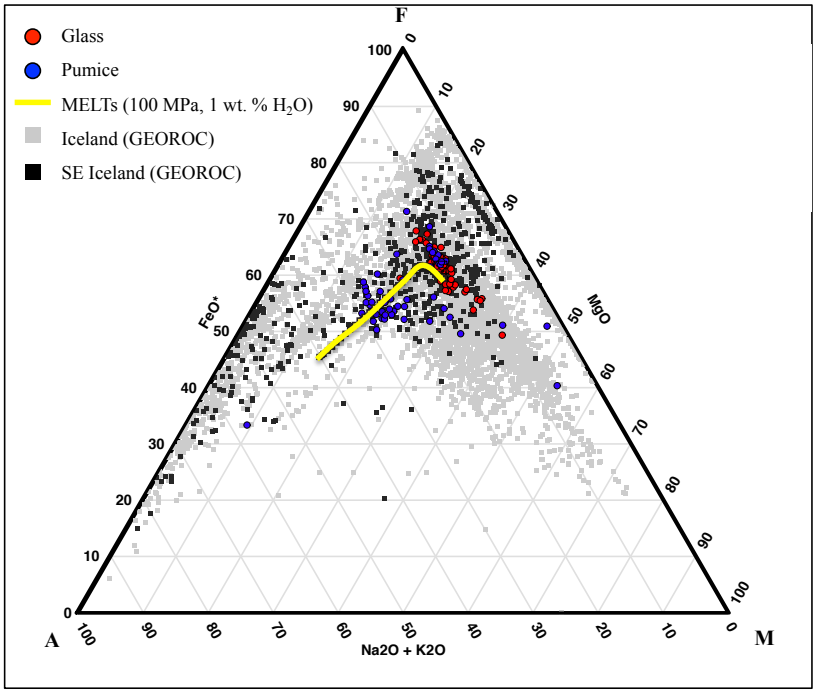

Figure 2: This AFM diagram is a compilation of: 50 glass shard analyses (red); 50 pumice fragment analyses (blue); all Icelandic whole rock and glass compositions compiled from the GEOROC database (gray); and Icelandic GEOROC data filtered for the southeastern quadrant of the country (black). The yellow line represents a MELTs modeling evolution path for a system with 1 wt. % water undergoing equilibrium crystallization at 100 MPa; the starting condition was above the liquidus with a starting composition of the glass analysis with the median SiO_2 value. All of our data (depicted in red and blue) was measured using FESEM-XEDS on detrital material separated from the Hverfisfljót River.

Mapping volcanoes in the Eastern Mexican Volcanic Belt: a natural laboratory

Gerardo Carrasco-Núñez[1], Mario Navarro[1], Javier Hernández [1] & Rodolfo Diaz[1]

Centro de Geociencias, Universidad Nacional Autónoma de México, campus Juriquilla, Queretaro, Mexico.

The Eastern Mexican Volcanic Belt (EMVB) includes a wide variety of contrasting volcanic structures ranging from large stratovolcanoes, calderas, and compound complexes to isolated domes, cinder and lava cones, maars, and even fisural activity, with compositions varying from basaltic to rhyolitic, with all types of deposits (scoria, large ignimbrites, avalanches, lahars, surge, fall, etc,) and eruptives styles (hawaiian, strombolian, vucanian, plianian, peleean, etc.), which in summary makes of this area a complete natural laboratory. We present a new map from the compilation the volcanic geology produced for several decades from detailed work in that region, which allow us to integrate all in a single map to show the diversity of volcanism in that area.

The EMVB comprises two different zones: the Cofre de Perote-Citlaltépetl Volcanic Range (CPCVR) and the Serdán-Oriental Basin (SOB). The CPCVR includes large composite volcanoes of dominantly andesitic-dacitic composition, including the shield-like compound Cofre de Perote, La Gloria and Las Cumbres complexes and the active but currently dormant Citlaltépetl (Pico de Orizaba) stratovolcano. This range represents an important physiographic divide having about 1 km in relief, which has promoted unstable conditions of the volcanic range producing repeated flank collapses toward the Gulf Coastal Plain during the last million year. The SOB is a closed basin in the high plains (2,300 m asl), featured by isolated monogenetic volcanism of Quaternary age and bimodal composition, with a minor proportion of Pliocene volcanoes, including isolated cinder and lava cones of basaltic composition, scattered rhyolitic domes and maar volcanoes, tephra rings and tephra cones. It is bounded to the north by the ~22 x15 km-diameter Los Humeros caldera, which has been active since ~0.46 Ma and have produced voluminous and widely distributed ignimbrites and fall deposits derived for caldera-forming eruptions. The SOB is dotted by small basaltic cinder and lava cones and larger rhyolitic domes (Las Derrumbadas twin complex), and towards the middle and south portions of the basin it includes also more than 10 maar volcanoes such as the multiple-vent Cerro Xalapazco tuff cone, Atexcac, Alchichica, Aljojuca and Tecuitlapa basaltic maars, Tepexitl rhyolitic tuff ring, Cerro Pinto dome-tuff-ring complex, most of them have circular crater shapes, but some others are elliptical and irregular, and some contain a crater lake inside. In addition of Citlaltépetl (Pico de Orizaba) stratovolcano other volcanic activity have occurred in Holocene times in the EMVB such as the pre-Columbian eruption of El Volcancillo at the northern flanks of Cofre de Perote and the recent reports of caldera-rim lavas from Los Humeros volcanic and Aljojuca crater. This recent activity have important implications for hazard assessment.

Titanomagnetite composition as a tool for geochemical fingerprinting andesitic tephra deposits from Mt. Taranaki, North Island, New Zealand

Magret Damaschke[1], Shane J. Cronin[1,2], R. Torres-Orozco[1]

[1] Institute of Agriculture & Environment, Massey University, Private Bag 11222, Palmerston North 4422, New Zealand, (M.Damaschke@massey.ac.nz), (R.Torres-Orozco@massey.ac.nz), R.C. Wallace1(R.C.Wallace@massey.ac.nz).
[2] School of Environment, University of Auckland, Auckland 1142, New Zealand, (s.cronin@auckland.ac.nz),

A c. 30,000 cal. yrs B.P.-long composite record of explosive eruptions from the andesitic stratovolcano, Mt. Taranaki, was established using titanomagnetite phenocrysts and volcanic glass shard compositions, in conjunction with precise age determinations of the tephra layers, from multiple lake and swamp sedimentary records. Titanomagnetite compositions are frequently unique to individual magmatic conditions and thus can be used in a similar way to compositional fingerprinting of glass. Based on these data, six different, geochemically distinct, stratigraphic tephra sequences have been defined: Tephra Sequence F (30 - 23.5 cal. ka B.P.), E (17.5 - 14 cal. ka B.P.), D (14 - 9.5 cal. ka B.P.), C (9.5 - 4 cal. ka B.P.), B (4 - 3 cal. ka. B.P.) and A (<3 cal. ka B.P.). These are the key to an unprecedented new view into the time-varying dynamics of Mt Taranaki, including any changes in geochemical composition, frequency and magnitude. Two distinct compositional trends are observed: (1) a broad evolutional trend from 17.5 to 3 cal. ka B.P. (Tephra Sequences E to B), and (2) an abrupt compositional change at c. 3 cal. ka B.P. (Tephra Sequence A), where basaltic tephras from Fantham's Peak, a parasitic cone on the flanks of Mt. Taranaki, interdigitate with andesitic tephras from the Summit. Further, geochemical analyses of key tephras from proximal sites on Mt. Taranaki were also performed, so now, for the first time, we can link the defined tephra sequences in lake and swamp environments with those on the upper flanks of the volcano. This not only helps resolve some previous stratigraphic issues, but also allows for the reconstruction of ash dispersal patterns, and calculations of eruption styles, column heights and volume estimates; all crucial to volcanic hazard assessments. The new findings not only provide a new firm basis for eruption hazard forecasting, but they highlight the complexity of this andesitic magmatic system and add fundamental new knowledge to the volcanic eruption record of Mt. Taranaki.

Degree of inertia versus forcing in pyroclastic currents and associated deposits

Domenico M. Doronzo[1], Guido Giordano[2]

[1] Centro de Geociencias, Universidad Nacional Autonoma de Mexico, Queretaro, Mexico, (doronzo@geociencias.unam.mx);
[2] Dipartimento di Scienze, Università di Roma 3, Roma, Italy, (ggiordano@os.uniroma3.it).

Pyroclastic currents in explosive volcanic eruptions are classically described between two end members, concentrated and dilute (Cashman and Sparks 2013, GSA Bull). Other very used terminology defines them as pyroclastic flow and pyroclastic surge, respectively (Cas and Wright 1987, book). Pyroclastic flows emplace massive-and-chaotic deposits, whereas pyroclastic surges emplace structured deposits, however lithofacies transitions can occur when one end member transforms into the other, depending on eruptive style (fountaining, blast, etc.) and topography (Sulpizio et al., 2014, JVGR). In order to bridge the two end members and account for their density-stratified nature, these currents are comprehensively defined as pyroclastic density currents (Branney and Kokelaar 2002, spec pub), following the models of concentrated and dilute subaqueous particulate currents. Recently, two new end members of pyroclastic currents, forced and inertial, have been proposed to account for the energy-stratified nature of the flow (Doronzo 2012, JVGR). Forced pyroclastic currents transport the total energy (combination of density, velocity and thermal energy) under the action of collapsing mass discharge rate, on steep slope or in channelized topography, i.e. driven (or forced) from outside the flow. Inertial pyroclastic currents transport the total energy by viscous or turbulent fluidization, i.e. from inside the flow. These new end members are based on sediment thermo-fluid dynamics, and do not substitute the classic terminology of pyroclastic currents. On the other hand, they allow to encompass the thermal effects, which are unique to pyroclastic currents among all natural gravity currents. Forced pyroclastic currents mostly emplace massive-and-chaotic deposits, but inertial pyroclastic currents do not necessarily emplace structured deposits. This is because of the energy-stratified nature of the flow, as inertia must increase with flow height (against gravity vector). For example, an ash cloud accompanying a pyroclastic flow may or may not decouple by inertia depending on topography, and the associated deposits (structured versus massive, respectively) will be affected by such possibility. The emplacement of the different layers in the pyroclastic deposit depends on the degree of inertia of the flow, which makes the emplacement of the whole deposit as a combination of progressive aggradation and en masse deposition (Giordano 1998, JVGR). This is because both transportation and deposition are subject to a balance between sediment and velocity fluxes within the current, which affects the final size of transportation (runout) and the onset of deposition (thickness) (Giordano and Dobran 1994, JVGR; Doronzo et al., 2012, JGR). In this sense, we suggest that the degree of inertia of a current can be described from the topological variations of deposit thickness with distance, which we call “topological aspect ratio” and is a new form of the commonly used

"regional" aspect ratio (sensu Walker et al., 1980, Nat), i.e. the simple ratio between a proxy for the total runout and the average thickness of the deposits. In this way, the thickening/thinning behaviour of ignimbrites may be related to the mode of transportation of the total energy within pyroclastic currents. For example, the deposits at high aspect ratio localities are massive-and-chaotic in response to poorer selection of the sediment, which occurs in a forced regime. The external influence, for example of a confined topography, on forced pyroclastic currents is testified by a reduced thermal interaction between the flow and the surrounding atmospheric air, and this can be inferred from the temperature of the deposits (e.g. Lesti et al., 2011, Bull Volcanol). Pyroclastic sequences of massive-and-chaotic deposits that have been interpreted with the forced flow end member are the ignimbrites of Tianchi Volcano, China (Chen et al., 2015, Bull Volcanol) and some ignimbrites of Cerro Blanco Volcanic Complex, Argentina (Báez et al., 2015, Rev Mex Sci Geol). Pyroclastic sequences that have been interpreted with the inertial flow end member are some other ignimbrites of Cerro Blanco Volcanic Complex, Argentina (Báez et al., 2015, Rev Mex Sci Geol) and the distal Plinian deposits of Mount Pelée, Martinique (Wright et al., 2016, GSA Bull).

Quantifying the Risk of Eruption for the Largest Volcano on Earth

Rachel Evans[1], Frank Trusdell[2]

[1] Shell; [2] SGS, HVO.

Mauna Loa is the world's largest volcano (Fig. 1, 2), covering more than half the Big Island in Hawaii at over 5000 km^2, and stands at 4170 m above mean sea level. It's also one of the most active volcanoes, having erupted 33 times since 1843, with the most recent eruption occurring in 1984. In 2004, 2009 and more recently 2014-16 volcano monitoring parameters have been recorded above background levels, leading to an increased risk Advisory/Yellow eruption status to be issued by the Hawaiian Volcano Observatory (HVO). Hazardous events evident during Mauna Loa's past eruptive history include extensive lava flows -travelling at distances up to 50 km and at speeds of up to 10 km/hr, ejection of pyroclastic material, expulsion of corrosive volcanic gases - SO_2, CO_2 & H_2S, roof collapse of lava tube chambers and landslides. In order to help anticipate future behaviour and identify potential hazardous areas, studies of the eruption history of Mauna Loa has been conducted by HVO since 1985, driven primarily in recent years by geologist Frank Trusdell. Quantitative refinement has enabled the production of a digital geological map using Geographical Information Systems software, focussing on volcano-hazard zones and the probability of lava flow inundation. Study methods used were mainly field-based (Fig.4), initially starting with desktop analysis of satellite imagery; identification of lava flow boundaries as well as structural features. Field work was then used to ground truth satellite interpretation; utilising techniques to conduct surface flow mapping, characterising mineralogical composition, and determining flow ages by radiocarbon dating and/or stratigraphic position. Fieldwork was supported by the use of ESRI's ArcPad software; formatted to digitally amend and map new lava flow boundaries whilst in the field, add gps waypoints and build a database of igneous rock sample mineral composition. Results are depicted in a 1:150,000 scale map of Mauna Loa volcano (Fig. 3) with > 500 surface lava flows historically dating back to 10,000 years of eruption history. A mapped inventory of spatial positioning of lava flows, physical volcanic features and associated relative age constraints, have enabled building an understanding of eruption cyclicity used to predict and de-risk future volcanic and earthquake hazards. The map is also used to indicate regions where landslides may preferentially occur; identify archaeological-cultural resources; provide a tool for locating threatened species, parent material for soil information and locating fresh water sources – rocks units which are preferential aquifers.

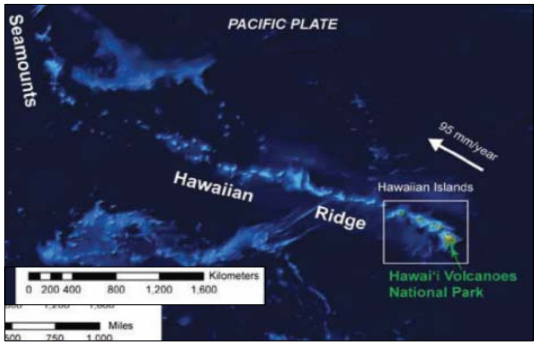

Fig.1 - *Location of the Big Island in the Hawaiian volcanic chain (Jason Jenworthy, NPS Geologic Resources Div, ESRI.* Fig. 2 - *Mauna Loa shield volcano (Jim Griggs, USGS, 1985).*

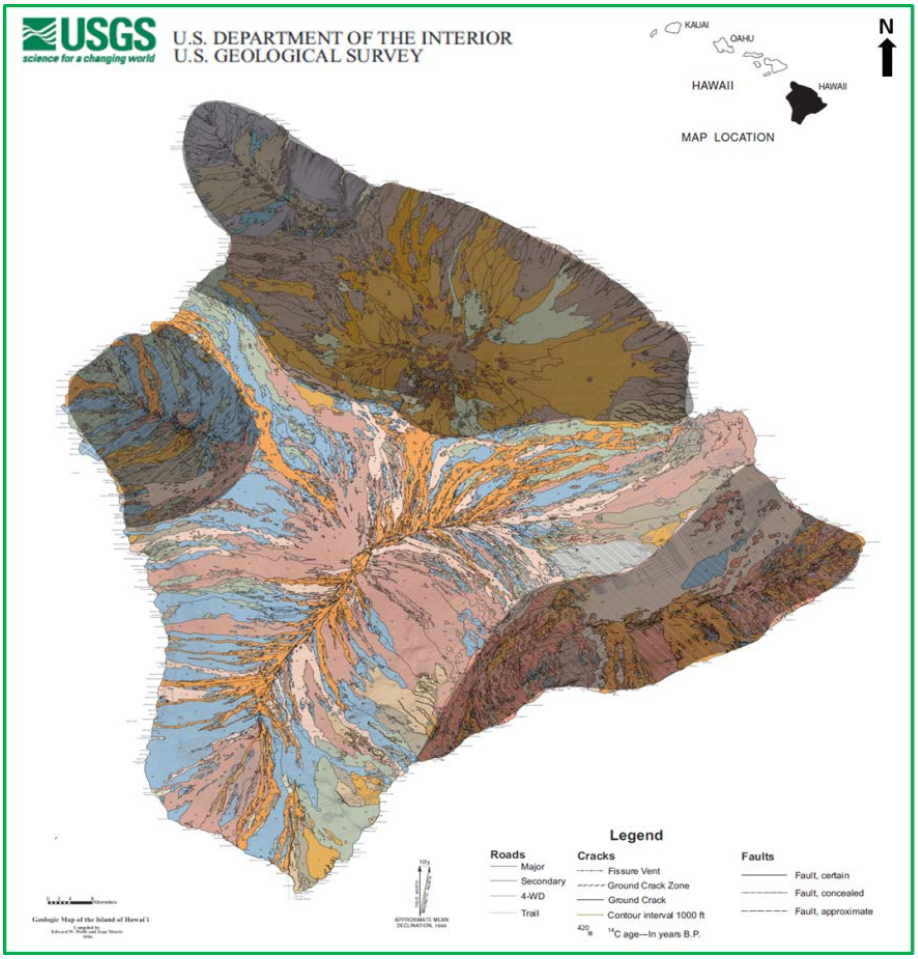

Fig. 3 - *Mauna Loa lava flows depicted by colour variations based on age (Digital Database of the Geologic Map of the Island of Hawai'I; Frank A. Trusdell, Edward W. Wolfe, and Jean Morris.*

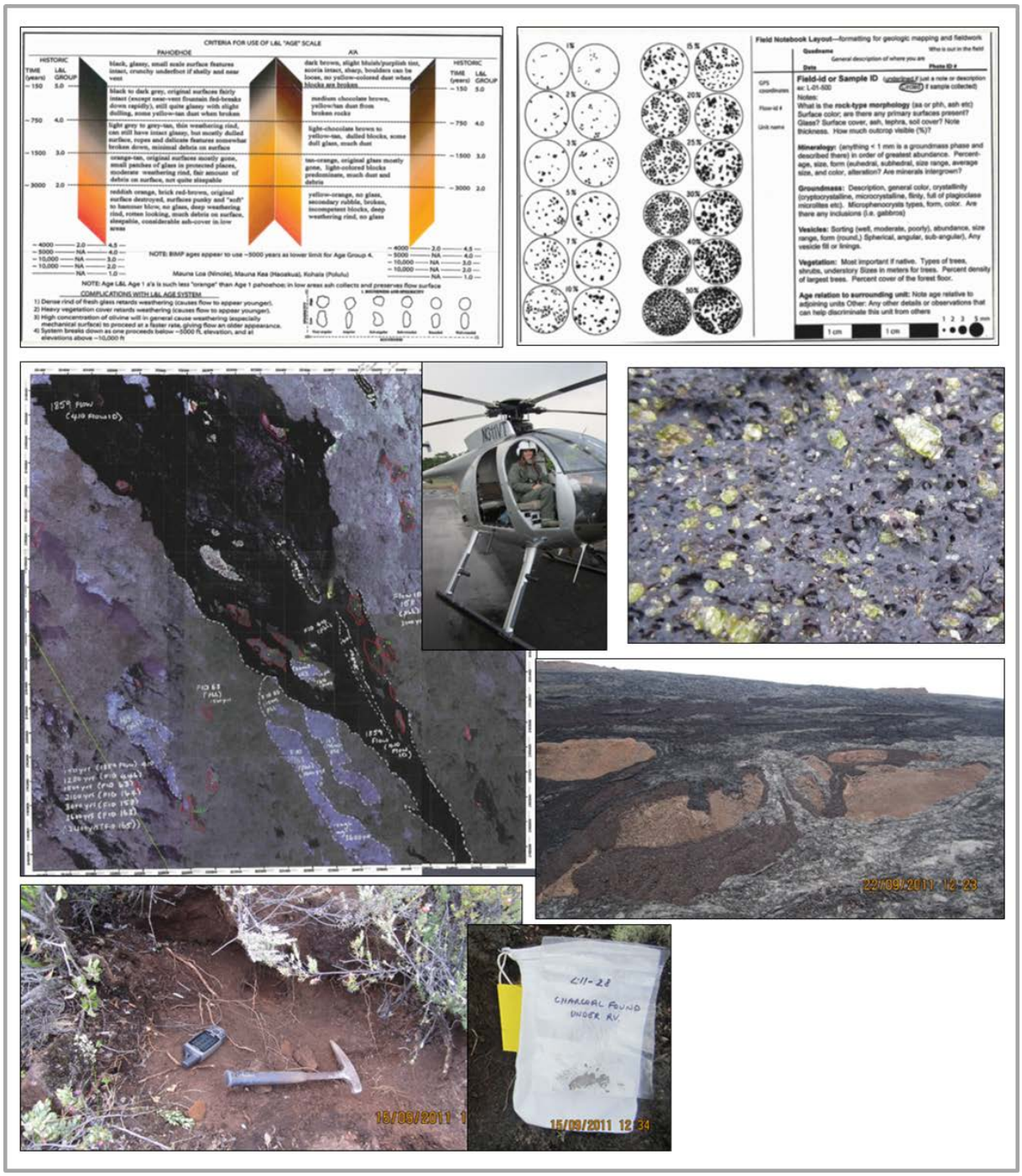

Fig.4 - *Pictorial overview of field-based methods & techniques used to map surface lava flows in designated regions on Mauna Loa volcano.*

Peach Spring Tuff (Southwestern, U.S.A.): Insights on Eruption Dynamics of a Remelted and Remobilized Silicic Cumulate

Michelle L. Foley[1] & Calvin F. Miller[1]

[1] Earth and Environmental Sciences, Vanderbilt University, 2301 Vanderbilt Place, Nashville, Tennessee 37235-1805, U.S.A., (michelle.l.foley.1@vanderbilt.edu and calvin.miller@vanderbilt.edu).

The ~1000 km^3 Peach Spring Tuff (PST) was the product of an 18.8 Ma supereruption, by far the largest within the Colorado River Extensional Corridor, Arizona-California-Nevada (e.g. Ferguson et al. 2013; Roche et al. 2016). It was erupted from Silver Creek caldera in the southern Black Mountains, AZ. PST outflow is predominantly crystal-poor, high-silica rhyolite (74-76 wt% SiO_2; Pamukcu et al 2013; Barry et al 2015). Ferguson & Cook (2015) identify five zones within outflow sections near Kingman, AZ. Although these zones are distinguishable on the basis of phenocryst, pumice and fiamme, and lithic content, the lower four are quite uniform in phenocryst and whole-rock compositions (Barry et al 2015). The distinctive uppermost unit, designated the Warm Springs zone (WSZ), is only locally exposed. Fiamme and pumice in this crystal-rich (~>35%), less silicic facies (trachyte – 65-69 wt% SiO_2) match intracaldera fiamme closely in texture and composition (Pamukcu et al. 2013; Foley et al. 2014). The crystal-poor outflow rhyolite and crystal-rich intracaldera and WSZ outflow trachyte have the same dominant phenocryst assemblage consisting of sanidine>plagioclase and biotite, accompanied by accessory magnetite, sphene, apatite, zircon, and chevkinite. Amphibole is also common in the crystal-poor rhyolite but rare within the crystal-rich trachyte, and very sparse quartz phenocrysts are also present in the rhyolite. Phenocrysts in trachytic pumice and fiamme are typically large (to several mm) and exhibit evidence of resorption and reaction, including heavily embayed and sieve textures. Where a contact between WSZ and underlying rhyolite tuff is exposed, it is marked by an abrupt decrease in lithics and increase in phenocryst content. Across the contact, welding changes from weakly-welded within the rhyolite tuff to densely-welded in WSZ; a vitrophyre horizon is generally present a short distance above the contact.Field evidence suggests that WSZ was the product of a discrete pulse following a time break post eruption of the previous four outflow zones – that is, it is a separate cooling unit. Previous geochemical, textural, and isotopic data support a model of the PST reservoir as a single, relatively simple, vertically stratified chamber with a crystal-rich base and massive, high-silica, crystal-poor upper zone (Pamukcu et al 2013; Frazier, 2013; McDowell et al. 2016). WSZ and the intracaldera trachyte represent the crystalline cumulate base proposed to have been partially remelted and remobilized, via injection of a hot mafic magma. We propose that the WSZ and intracaldera tuff tapped the same bottom-of-chamber material after a brief hiatus in the PST eruption, possibly accompanying and following caldera collapse.

Lava emplacement in Al-Lajā' (Syrian Hauran): The longest lava tube in the Levant

Amos Frumkin

Institute of earth Sciences, The Hebrew University, Jerusalem, Israel 91904, (amos.frumkin@mail.huji.ac.il).

When a lava tube is near the surface, sections of its roof may erode or collapse, creating a 'puka' or 'skylight' holes in the roof, as well as elongated unroofed caves. The continuous nature of such partially collapsed lava tubes and/or lava channels can thus be identified by remote sensing as 'dashed lines' of intact lava tube segments, pits, and channels, collectively referred to as a 'lava tube system'. The intuitive and easy-to-use Google Earth with its improved SPOT Images has rapidly emerged as a global medium with increasing potential for lava tube prospection, outflanking other types of orbital imagery and remote-sensing sources. The largest volcanic region of the Levant is Harrat Ash-Shaam, covering some 40,000 km^2 in Syria, Jordan, Saudi Arabia, and Israel. Several lava tubes are known in its northeastern area, the Hauran, all of them are thought to be of Quaternary age. Tawk et al. (2009) reported a 562 m long, 21 m wide, 4 m high lava tube in Ariqa village, NE of Jabal ad-Druze. This region of Harrat Ash-Shaam, called Al-Lajāʾ ('refuge'), is covered by rough late-Quaternary basalt, with limited human access. Here I report that Ariqa Cave is a small portion of the longest lava tube system in the Levant.

The lava tube system is identified by its remotely sensed collapsed segments, forming an elongated line of troughs. These troughs are either unroofed lava tubes, or open lava channels, inferred by what seems to be lava levees. The relief of the channels is emphasized by the typical shade of its southern wall. In addition, the channel/collapsed segments act as sediment traps, which become natural 'flowerpots' supporting denser vegetation, compared with the surrounding rocky lava. Some topographic troughs of the lava tube system are large enough to be indicated on topographic maps. A corroboration for the existence of an uncollapsed lava tube segment is given by the cave survey (Tawk et al., 2009), as well as cave attributes on topographic maps, where all are aligned along the inferred lava tube system. The topographic maps, based on photogrammetry, show clear trenches, which are segments of collapsed lave tubes/channels. In addition to Ariqa Cave, two unexplored lava tube caves are indicated on topographic maps east of Ariqa: Meg'arat Hamid and Meg'arat a-Shatab. Additional segments of the lava tube system are observed on Google Earth imagery but not on topographic maps. The lava tube segments are compiled and reconstructed from all the above mentioned data. The entire system is 20.5 km long, descending from 890 to 650 m a.s.l., in a mean gradient of 1.2%. It spans most length of the recent pahoehoe lava field that flowed westward from Tel Shihan region,shedding light on the lava emplacement mechanism.

Phreatomagmatic explosive eruption in high stratovolcanoes triggered by lateral fissure propagation: Examples from Mt. Etna and Miyakejima

Nobuo Geshi[1], Karoly Nemeth[2], Marco Neri[3]

[1]Geological Survey of Japan, AIST (geshi-nob@aist.go.jp); [2] CS-IAE, Volcanic Risk Solutions, Massey University; [3] Istituto Nazionale di Geofisica e Vulcanologia, Osservatorio Etneo.

Lateral propagation of feeder dike from summit to flank in stratovolcano can result explosive phreatomagmatic eruption in the summit part of the stratovolcano. Here we present two examples of phreatomagmatic explosive activity in the final stage of the fissure eruption in a large stratovolcano. The 1809 AD flank eruption in the North East Rift of Mt. Etna, Sicily, formed a chain of explosion craters in the upper portion of the eruption fissure. The eruptive activity in the upper portion of the fissure started with fire fountain with very-limited influence of external water. Then the eruption fissure propagated downward in the flank area to feed a large lava flow. The eruptive activity in the upper segment shifted to explosive phreatomagmatic activity as the propagation of eruptive fissure to the lower flank. Shift from dry magmatic eruption to phreatomagmatic explosions also recognized in the 7th Century Suoana-Kazahaya fissure eruption in Miyakejima, Japan. The proximal deposit shows that the eruption started with vigorous fire-fountain in the uppermost portion of the eruption fissure in the northern corner of the summit. The eruption fissure propagated downward and reached to the lower-flank area. Activity in upper portion of the fissure changed to explosive phreatomagmatic eruption as the propagation of the eruption fissure. Transition from magmatic to phreatomagmatic occurred only in the upper half of the eruption fissure, including the Suoana crater, whereas the lower half of the fissure continued dry magmatic eruption throughout their activity. The transition from magmatic eruption to phreatomagmatic explosive activity observed in both cases indicates that the magma-water interaction started at the middle of the eruption. The limited distribution of phreatomagmatic activity in the upper eruption fissure can be resulted by the magma extraction from the upper feeder dike system to the lower eruption fissure as it contributed to the general drop of magmatic pressure in the upper section of the fissure-fed conduit. The drop of magma flux resulted the access of ground water was able to access the still hot feeder dikes and initiate phreatomagmatic explosive eruptions. The existence of buried summit caldera that can host large quantity of groundwater also contributes the limited distribution of phreatomagmatic activity in the summit area.

The complexity of volcanic lithofacies of the Quaternary silicic Puketerata tuff ring-lava dome complex and its implication to define lithostratigraphic units associated with pre-Quaternary successions

Szabolcs Kósik, Károly Németh

Institute of Agriculture and Environment, Massey University, Palmerston North, New Zeland, (s.kosik@massey.ac.nz k.nemeth@massey.ac.nz).

Definition of lithostratigraphic units in volcanic terrains is particularly challenging as they can be associated with different volcano-sedimentary processes. Their physical characteristics used to define features applied for mapping purposes that can inherit information on the magma fragmentation, vesiculation, crystallisation, pyroclast transportation, deposition and resedimentation. This problem is enhanced by the shifting of vents. In long-lived volcanic systems, polygenetic volcanoes can grow and produce lithostratigraphy units that follow the distinction of eruptive units that results pyroclast accumulation in eruptive phases and related syn-eruptive resedimentation during a single eruptive episode (month to years). The deposits of eruptive episodes accompanied with post-eruptive resedimentation form tephra units of fast accumulating primary deposits interbedded with resedimented deposits. An eruptive period can last many years to millennia leaving behind a primary and reworked pyroclast succession that can be associated with lithological features that are practical for mapping. Eruptive periods are in such volcanic systems can host major landscape forming mappable zones closely resembling unconformity hence an eruptive period could be expressed in a single unconformity bounded unit. In polygenetic volcanic systems lithostratigraphic units are reasonable easy to define, while when a volcanic system is composed of small-to-medium size volcanoes problems are common in unit definition and identification. Mapping of pre-Quaternary successions are even more problematic due to information. The 14 ka Puketarata eruption in the Taupo Volcanic Zone in New Zealand produced a lava dome-dominated edifice that is confined within a silicic tuff ring showing laterally quickly changing facies characteristics.

The basal succession of the tuff ring consists of ash and lapilli ash beds dominated by textural features typical for traction sedimentation from a horizontally moving coherent (wet/moist current) pyroclastic surge interbedded some coarse grained angular lapilli rich layers. These layers indicate intermittent and coeval air fall of larger clasts derived from an expanding column excavating clasts from a crater hosted a lava dome. This basal unit is covered with sedimentary contact by a stratified and partially cross bedded ash and lapilli unit more typical for dry magmatic explosive eruptions. This unit is also accompanied with several air fall beds among one deposited particularly thick lapilli bed in proximal areas. The succession subsequently covered by another unit similar to the basal unit however its thickness is larger. The entire succession is capped by angular lava-dome derived lapilli and block dominated fine matrix hosted pyroclastic succession indicating a late stage lava dome growth that culminated in a lava dome collapse.

This deposit also hosts some air fall beds of ash. The overall unit distribution around the crater however from the median distances (~500 metres) show dramatic facies variations of preserved tephra layers that best to interpret as a result of the combination of 1) vent migration as some elongated depression still can be recognized over 700 m length, 2) rapid changes in accumulating tephra thickness of air fall origin ash, 3) topographical effect to control the accumulation pattern of pyroclastic density current-deposited ash. These above listed three parameters created a facies association that can be grouped in a single package in more medial to distal regions as the representation of a tephra unit that composed of individual eruptive phases with very little sign of having even syn-eruptive resedimentation.

The lateral facies variation of Puketerata is striking, however, the obviousness of treating its eruptive products as a mapping unit is clear as defining it as a tephra unit. The case of Puketerata however raise some questions how to apply the lithostratigraphical approach and to interpret similar dome-related sequences in older settings especially if such volcanism is the main type of volcanism of the region as it is the case in many Miocene arc-related silicic volcanic systems along the Carpathian Volcanic Arc in Central Europe. Volcanic region such as those of the Tokaj Mountains in NE Hungary and SE Slovakia hosts numerous Miocene rhyolitic, rhyodacitic eruptive products that sourced dominantly from small-to-medium sized lava domes commonly sitting on/in and intercalated with some major basin-wide ignimbrite products sourced from regional volcano-tectonic calderas, similar to those located in the Taupo Volcanic Zone and hosts Puketerata. In the case of Puketerata, in a Quaternary volcano, it is easy to distinguish the Puketerata-derived tephras even in medial or distal settings from a soil covered post eruptive resedimented succession developed on the surface of an older ignimbrite of the Maroa Volcanic Center (Whakamaru caldera). In the Miocene Tokaj Mountain however, lava domes and their pyroclastic successions can be defined in their proximal areas while in distal regions the tephras can be missing and/or just not recognized due to similarities in composition with their under and overlying units causing difficulty to group them in a mapping unit. To overcome this problem in pre-Quaternary settings a detailed lithological analysis including a paleovolcanic and environmental interpretation is essential to define mappable volcanic lithostratigraphic units closely resembling an “unconformity bounded” units distinct from their base and top successions along petrological, petrographical and sedimentological aspects.

This process however not obviously needs to be governed by identification of unconformities as especially in inter-edifice regions with steady background sedimentation a complex pile of primary and reworked tephra successions can be accumulated from different sources interfingering tephras and reworked equivalents forming lithostratigraphy units typically develop from each other through sedimentary contacts as it has been the case in Puketerata. A definition of lithostratigraphic units, especially in pre-Quaternary silicic volcanic terrains, should also consider the scale of observation. In a period of only few millions years in history of silicic volcanism multiple pyroclastic units with near-identical physical appearance can mimic a basin-wide single lithostratigraphy unit.

Distinction between locally sourced and multiple event derived deposits from single sourced and single event-related horizons hence is important and geologically valid approach as it has been demonstrated in the Quaternary Puketerata section.

Mapping of the lava field of the Paricutin historical eruption

Patricia Larrea[1], Elisabeth Widom[1], Claus Siebe[2], Sergio Salinas[2], Robbyn Abbitt[3], David Kuenz[1]

[1]Department of Geology and Environmental Earth Science, Miami University, Oxford, 45056, U.S.A., (larreap@miamioh.edu; widome@miamioh.edu; kuentzdc@miamioh.edu); [2]Departamento de Vulcanología, Instituto de Geofísica, Universidad Nacional Autónoma de México, Ciudad Universitaria, C.P. 04510 Coyoacán, México D.F.,(csiebe@geofisica.unam.mx; sss@geofisica.unam.mx); [3] Department of Geography, Miami University,Oxford, Ohio 45056, U.S.A., (abbittrj@miamioh.edu).

Paricutin is the youngest volcano of the Michoacán-Guanajuato volcanic field (MGVF) in the Trans-Mexican Volcanic Belt (TMVB). It is located ~320 km west of Mexico City at latitude 19°29'35″N and longitude 102°15'05″W. The MGVF contains more than 1,400 volcanic edifices, including monogenetic scoria cones, shield volcanoes, and maars (Hasenaka and Carmichael, 1985; Hasenaka et al., 1994) formed in relation to the subduction of the Rivera and Cocos plates beneath the North American plate. Paricutin (AD 1943-1952) and Jorullo (AD 1759-1774) are the only two monogenetic volcanoes in the TMVB born in historic times, being entirely formed by the eruption of a small volume of mafic magma. The eruption of Paricutin volcano started in a corn-field on the 20th of February 1943 and ended 9 years later on the 4th of March 1952 (Luhr and Simkin, 2003). After intense explosive activity during the first year, the average rate of magma emission decreased gradually with time until the eruption ended, covering a total area of 233 km^2 (Segerstrom, 1950) with ~1.38 km^3 of lava and pyroclastic material (Fries, 1953; McBirney et al., 1987). Paricutin represents one of the rare occasions when scientists had the opportunity to observe the birth of a new volcano and document its entire eruption. The eruption caught the attention and interest of scientists all over the world, making this volcano one of the most outstanding examples for understanding the origin and evolution of monogenetic eruptions. Geologists from different institutions, including the U.S. Geological Survey and the Universidad Nacional Autónoma de México surveyed all of the eruptive phases in progress. They wrote detailed descriptions, mapped the lava flows, and took samples and photographs during the nine years of eruptive activity. In particular, the geologists Adan Pérez-Peña, William Foshag, and Ray Wilcox sketched tephra and lava distributions throughout the eruption, providing maps depicting the volcano's sequential growth. More recently, Luhr and Simkin (1993) compiled all of the published works and defined 23 eruptive stages by date of eruption (Fig. 1).

GIS software has become a valuable tool for geologic map preparation, and expertise in this software is nowadays a necessary skill for geoscientists. Moreover, in recent years the methodologies used in geologic fieldwork data collection, analysis, and mapping have changed due to the incorporation of global positioning system (GPS) and geographic information system (GIS) equipped mobile devices (i.e., tablets and cell phones) (e.g., Whitmeyer and Nicoletti, 2010; McCaffrey et al., 2005, and references therein). In this work, we present the new methodological approach, which utilizes these recent technological advances, used in our 2015 fieldwork

campaigns to identify the Paricutin eruptive stages as originally defined by Luhr and Simkin (1993). We first scanned and georeferenced the maps of all of the 23 eruptive stages (Luhr and Simkin, 1993; Fig. 1) using ArcGIS (ArcMap 10.3). Once all of the lava flows were digitized, the map created in ArcMap was uploaded to the Miami University ArcGISOnline cloud. The Collector for ArcGIS App, which can be installed on any smartphone or tablet device, allows for viewing and interaction with the map when offline during the fieldwork campaign. The App uses the GPS signal of the mobile device to indicate the user's real-time location on the map, confirming one's exact position on the eruptive deposits of any given stage required for sampling. This new field methodology facilitated the identification and sampling of all exposed Paricutin eruptive stages, which is required for our ongoing comprehensive geochemical study of Paricutin (Larrea et al., in preparation). In addition, we are pursuing a volumetric study of the entire lava field sequence combining the GIS data with pre- and post-eruption digital elevation models. Together, these studies will provide the first comprehensive documentation of the combined chemical-temporal-volumetric evolution of the Paricutin volcanic system.

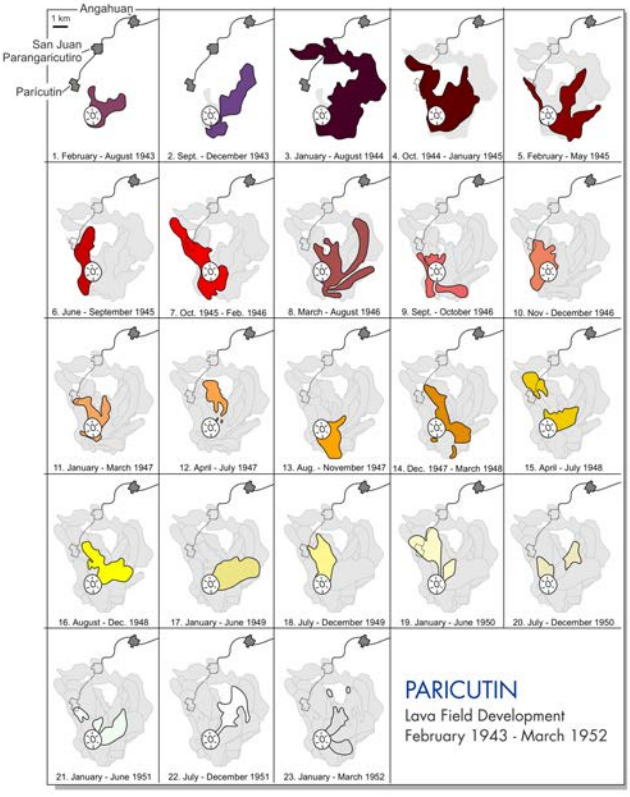

Fig. 1 - *Summary of the Paricutin lava field development, representing the 23 defined lava flow eruptive stages (modified after Luhr and Simkin, 2003). Each eruptive stage is defined by a map sketched at the time of the eruption, which delimits the area covered by that particular eruption, and the previous extension of the lava field. Note that each map contained at least one coordinate point that was key for the geo-referencing process of the eruptive stages in GIS.*

References

Fries C. (1953). Volumes and weights of pyroclastic material, lava and water erupted by Paricutin volcano, Michoacán, Mexico. Transactions of the American Geophysical Union, 34 (4): 603-616.

Hasenaka T. and Carmichael, I.S.E. (1985). The cinder cones of Michoacán-Guanajuato, Central Mexico: Their age, volume and distribution, and magma discharge rate. Journal of Volcanology and Geothermal Research, 25: 105-124.

Hasenaka T., Ban, M., Delgado-Granados H. (1994). Contrasting volcanism in the Michoacán-Guanajuato volcanic field, Central México: Shield volcanoes vs. Cinder cones. Geofísica Internacional, 33(1): 125-138.

Luhr J.F. and Simkin T. (2003). Paricutin. The Volcano Born in a Mexican Cornfield. Geoscience Press, Phoenix, 427 pp.

McCaffrey K.J.W., Jones R.R., Holdsworth R.E., Wilson R.W., Clegg P., Imber J., Holliman N., Trinks I. (2005). Unlocking the spatial dimension: digital technologies and the future of geoscience fieldwork. Journal of the Geological Society, 162:927-938.

McBirney A.R., Taylor H.P., Armstrong R.L. (1987). Paricutin re-examined: a classic example of crustal assimilation in calc-alkaline magma. Contributions to Mineralogy and Petrology, 95:4-20.

Segerstrom K. (1950). Erosion studies at Paricutin volcano, state of Michoacán, Mexico. U.S. Geological Survey Bulletin, 965A:1-164.

Whitmeyer S.J. and Nicoletti J. (2010). The digital revolution in geologic mapping. GSA Today, 20(4):4-10.

Voluminous early Miocene volcanism in the Southern Black Mountains, Arizona, USA

Calvin F. Miller[1], Susanne M. McDowell[1], Michelle L. Foley[1], Jonathan S. Miller[2], Lily L. Claiborne[1], & Nicholas P. Lang[3]

[1]Earth and Environmental Sciences, Vanderbilt Univ., Nashville, Tennessee 37235, U.S.A., (calvin.miller@vanderbilt.edu; susanne.m.mcdowell@gmail.com; michelle.l.foley.1@vanderbilt.edu); [2] Geology, San Jose State University, San Jose, CA 95192-0102, U.S.A., (jonathan.miller@sjsu.edu; lily.claiborne@Vanderbilt.Edu); [3] Geology, Mercyhurst University, Erie, PA 16546, U.S.A., (nlang@mercyhurst.edu).

At the onset of extension at 35° N in the Colorado River rift, Arizona-California-Nevada, the southern Black Mountains were a major locus of volcanism that lasted from ~19.5 to 17 Ma (McDowell et al. 2014, 2016). Mafic to felsic lavas and tuffs were accompanied by extensive dikes, sills, and shallow stocks. Thick lava sequences document a dominantly effusive eruptive history, with the notable exception of the super-eruption scale (~1000 km^3 d.r.e.), dominantly high-silica rhyolite Peach Spring Tuff (PST), whose source caldera lies in the center of the southern Black Mountains (Ferguson et al., 2013; Pamukcu et al., 2013). Prior to the 18.8 Ma PST eruption, almost all eruption products were intermediate in composition, primarily trachyte and trachydacite with minor trachyandesite and trachybasalt. One large ignimbrite, the trachytic Cook Canyon Tuff (>10 km^3), and several small pyroclastic eruptions accompanied the voluminous lavas. Total volume of the pre-PST eruption deposits was roughly 2000 km^3. Following PST, lavas, lava domes, block-and-ash flows, and lesser ash falls and flows erupted, all relatively small in volume (<10 km^3). Compositions of the post-PST eruption products spanned a broad compositional spectrum, from trachybasalt through trachyandesite and trachydacite to dominant rhyolite.

A common theme of magmatism in the southern Black Mountains is the subtle but seemingly important signature of primitive, relatively mafic magma in an intermediate to felsic eruptive regime. Lavas with less than 60 wt% SiO_2 are sparse and small in volume, but dikes and sills of this composition are fairly widespread, enclaves are present throughout the volcanic section, and evidence for mingling with mafic to intermediate magma is abundant in the shallow granitic intrusions (McDowell et al 2014). Notably, mafic magmatic enclaves are a very minor but persistent constituent of the PST (Pamukcu et al., 2013; Flansburg et al., 2015). Zircon saturation and Ti-in-zircon thermometry (Boehnke et al., 2013; Ferry and Watson 2007), Rhyolite-MELTS modeling (Gualda et al., 2012), and Zr/Sr ratios (Miller et al., 2014) all point to high temperatures for the relatively silicic magmatism in the southern Black Mountains, generally >/= ~800° C in rhyolites and reaching 1000° C or more in some trachyte lava (McDowell et al 2014; Pamukcu et al., 2013; Flansburg et al., 2015). The PST eruption appears to have coincided with a thermal maximum, and the base of its rhyolitic magma chamber was heated to T approaching or exceeding 900° C prior to eruption (Pamukcu et al., 2013; Foley et al.,2014; Foley and Miller 2016, this conference).

Eruption flux also was at a maximum through PST time and diminished considerably afterward (~$4*10^{-3}$ km^3/yr from ~19.5-18.8 Ma, ~$3*10^{-4}$ km^3/yr from 18.8-17 Ma). Despite generally higher temperatures prior to PST and more silicic compositions after PST, whole-rock and zircon isotopic ratios (Nd, Hf, Sr, Pb, O) point to a larger mantle component in post-PST volcanic and plutonic rocks. Isotopic compositions are generally heterogeneous on mineral (zircon) and whole-rock scale, consistent with field and textural evidence for open-system processes. The PST has both the most homogeneous and the most evolved (crustal) isotopic composition (McDowell et al 2016; Frazier 2013; Overton 2014). Prior to 19 Ma, dominant volcanism in the Colorado River rift occurred to the south of the Black Mountains. After 17 Ma, the primary locus of eruption shifted northward, from the study area to the central and northern Black Mountains (Varga et al., 2004; Faulds et al., 2001, 2002). Compositions and eruptive styles during the easrlier and later phases mimicked those in the southern Black Mountains, except that no other eruption within the rift ever approached the magnitude of the PST.

Geophysicists searching for volcanoes . . . and mapping them

Jan Mrlina

Institute of Geophysics ASCR, Boční II 1401, Prague 4, 141 31, Czech Republic, (jan@ig.cas.cz).

There is so many things to be investigated by volcanologists on volcanic structures. However, it is still difficult, if not impossible, to image deeper subsurface of those structures. There are also volcanoes still hidden and unknown due to no visible expression in topography, especially eroded scoria cones or maars. We propose, based on experience, to apply geophysical mapping for the search of undiscovered volcanoes, as well as for more detailed investigation of the interior of volcanic bodies.

From various geophysical methods I suggest gravity and magnetics for general search and mapping. It has been proved many times that volcanic structures give origin to impressive, or at least well recognizable gravity anomalies, usually gravity lows of a few mGal (10-5 m/s2), which is two order higher than the resolution of gravity instrumentation. Gravity lows are caused by any sort of unconsolidated volcanic products, as breccias, lapilli, dust, scoria, tuff, tephra, etc. Not only the rock can actually be the source of anomalies, but also the structure itself with country rock disintegration, low density fill composed of both back-fallen eruption products and younger (lake) sediments, as in case of maars.

Long ago, we identified a volcanic structure during the gravity mapping in the scale 1:25.000 where a single point with negative anomaly gave origin to a detailed survey discovering a small complex volcano. The structure was located in a negligible topographic depression, with no real indication as for morphological shape (Mrlina et al., 1989). Similarly, but under different 'work flow' we discovered an unknown hidden Quaternary maar structure in Western Bohemia, where we had a chance to confirm the finding by an exploration drilling to 85.5 m depth, just to catch breciia with some volcanic bombs under the cover of 84 m of young sediments (Mrlina et al., 2007, 2009).

Magnetics can locate volcanic structures in case they consist of intermediate and basic rocks like basalts s.l. However, this technique will provide an image of all magnetic products of eruption/effusion/flows around the volcano, so that the amount of such products can be mapped and quantitatively estimated. Such image is shown in Fig. 1, where the central magnetic anomaly shows a maar structure filled by sediments and breccias, but the other striking anomalies reflect extensive volcanic products in the surroundings of the structure. This image was produced by 'extracting' significant anomalies from the usual contour map using special multiple-filtering processing. The magnetic image is superimposed over a shaded gravity map, so that the gravity low of blue color is less visible, but the other features are present in the image. In general, positive anomalies are related to most of the volcanic structures due to high content of magnetic minerals in the volcanic rocks (except acid trachytes/phonolites).

There may be other techniques applied as well to enhance the internal structure, like resistivity tomography, shallow seismic, but also seismology in case of an active volcano. But this is already not mapping, but monitoring.

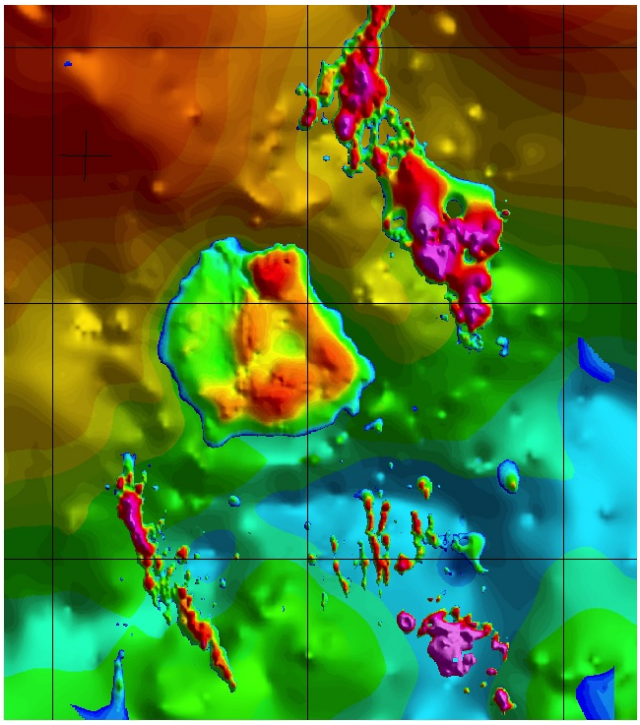

Fig. 1 - *Mytina Maar – extracted magnetic anomalies indicate the main structure anomaly in the centre, as well as other volcanic products deposited in the surrounding (tephra); in SW we do not exclude the presence of a dike. The violet anomaly in SE is actually a scoria cone of a small volcano.*

References

Mrlina J., Kämpf H., Geissler W.H., van den Boogart P., (2007): Assumed Quaternary maar structure at the Czech/German boundary between Mýtina and Neualbenreuth (western Eger Rift, Central Europe): geophysical, petrochemical and geochronological indications – Z. geol. Wiss., 35, 4-5: 213-230.

Mrlina J., Kämpf H., Kroner C., Mingram, J., Stebich M., Brauer A., Geissler W.H., Kallmeyer J., Matthes H. and Seidl, M. , 2009): Discovery of the first Quaternary maar in the Bohemian Massif, Central Europe, based on combined geophysical and geological surveys. – J. Volc. Geoth. Res. , 182, 97-112. DOI: 10.1016/j.jvolgeores.2009.01.027

Mrlina J., Pospíšil M., Peška P. (1989): Geophysically disclosed occurrence of neovolcanites near Dobra Voda (Tepla Crystalline complex). - Věst.Ústř.Úst.geol.,64, 6, 353-362, Praha.

Subsurface mapping: volcanic fissure geometry at Kilauea

Carolyn Parcheta, Aaron Parness, Karl Mitchell, Jeremy Nash

Jet Propulsion Laboratory, California Institute of Technology.

Volcanic fissure vents are difficult to quantify due to their inherent danger and their extremely narrow size. Additionally, lava flows, lava drain back, or collapsed rampart blocks typically conceal a fissure's surface expression. When a fissure remains exposed, subsurface mapping the non-uniform distribution of wall irregularities, drain back textures, and the larger scale sinuosity of the whole fissure system can be done with VolcanoBot. Mapping occurs after the fissure ends activity and cools off to < 50º C. The robot uses a near-IR structured light sensor that can reproduce the 3d structure to cm-scale accuracy. Here we present a portion of our 3D model within the Mauna Ulu fissure system. We see a self-similar pattern of irregularities on the fissure walls throughout the entire shallow subsurface, implying a fracture mechanical origin. These irregularities are typically 1 m across, protrude 30 cm into the drained fissure, and have a vertical spacing of 2 m. The size of these irregularities is variable and distinct with depth, potentially reflecting stratigraphy in the wall rock hosting the fissure system. Irregularities are larger than the maximum 10% wall roughness used in engineering fluid dynamic studies, indicating that magma fluid dynamics during fissure eruptions are probably not as passive nor as simple as previously thought. Where piercing points are present, we infer the dike broke the wall rock in order to propagate upwards; where they are not, we infer that syn-eruptive mechanical erosion has taken place.

This work is funded by a NASA Postdoctoral fellowship through University Space Research Association. This work was performed at the Jet Propulsion Laboratory/California Institute of Technology under a contract with NASA.

Facing geological mapping in low-latitude volcanoes: Doña Juana Volcanic Complex study-case, Colombia

Natalia Pardo[1,2]*, Bernardo Pulgarín[1], Valentina Betancourt[1], Federico Lucchi[3]

[1] Volcano Geology Team at Servicio Geológico Colombiano (*n.pardo@uniandes.edu.co); [2] Departamento de Geociencias, Universidad de Los Andes, Bogotá-Colombia; [3] Dipartimento di Scienze Biologiche, Geologiche e Ambientali, Universitá di Bologna-Italia.

Significant efforts on establishing a coherent method to develop geological maps and stratigraphy of volcanic environments have been made in the last decades. The peculiarities of working in volcanic areas, compared to other sedimentary settings, derive from their extremely dynamic transport-and-depositional regimes, rapid landscape modification, multiple, and often simultaneous, vents of variable geometry and location, as well as dramatic hydrogeological changes, and abrupt lithofacies variations. The episodic nature of volcanic eruptions and the catastrophic character of events, such as caldera-and-sector collapses, capable of changing the geometry and position of the reservoir-plumbing-vent system, pose serious challenges for geological mapping and stratigraphic correlation. The recently established IAVCEI Commission on Volcano Geology has been an encouraging strategy to link researchers interested in discussing fieldwork techniques, and to develop best practices to reinforce the use of the geological record, as the basic data-source for understanding volcanic behaviour and hazard assessment. In the last few years, an innovative methodology integrating traditional lithostratigraphy and lithofacies analysis (for mapping), lithosomes (for the definition of eruptive centres), unconformity-bounded units, and geochronology (for stratigraphic correlation), as well as the definition of eruption units (for interpretation and quantification of the eruptive history), has been discussed. However, most of the examples supporting its practical applicability have been carried on at high-latitude and Mediterranean volcanoes, with climatic conditions distant from the equatorial regions.

Therefore, this project aimed to evaluate the utility of the discussed method in densely vegetated volcanoes, subject to frequent and heavy precipitation; such equatorial volcanoes are commonly surrounded by densely populated areas in developing countries, where vulnerability is relatively high, and the acquisition of objective and complete geological data for hazard evaluation is usually complicated. Doña Juana Volcanic-Complex (DJVC) is located in SW Colombia (1°27'-1°34'N y 77°3'- 76°54' W), mainly emplaced over Lower Cretaceous, metasedimentary and volcanic rocks of oceanic affinity, within the Central Cordillera of the Colombian Andes. DJVC has mainly emitted calc-alkaline, mid-K_2O, dacitic magmas, resulting in variable, high-viscosity volcanic products, including lava-domes, which currently reach 4150 m above-sea-level. Following a first geomorphological analysis, using satellite images, a 12 m DEM, an Arc-GIS generated slope-map, air-photography, and taking into account previous and new field studies, first, second, and third-order unconformities were identified.

The hierarchy of the unconformities was established according to their areal distribution, following 1:10.000-1:25.000 field-work, and optimizing its presentation on a 1:50.000 map. Thus, synthems were defined, which include lithosomes (internal and external), and lithostratigraphic units of known lithology, lithofacies architecture, basal contacts, relative stratigraphic position, and distribution; for some of these units, C^{14} absolute ages were available. However, in contrast to high-latitude volcanoes, within Colombian equatorial-climate conditions, the correlation of such unconformities requires an interpretative component because of the dense vegetation, abrupt topography, and the national armed conflict; also, informal geomorphological units (distinguished with remote sensors but inaccessible in the field), and other informal lithological units (i.e., of known lithology but unknown age and lacking precise correlation) needed to be used. Moreover, besides traditional tephrostratigraphic methods, well-developed, widespread paleosols were taken into account for subdividing Holocene formations into members and call the attention on potential repose-periods or significant decreased intensity in the volcanic activity.

Finally, eruption units were interpreted, as well as the transport-and-emplacement mechanisms responsible for the resulting geological record, based on their lithofacies associations, which are the primordial source for hazard evaluation purposes. In general, the discussed method could be applied, although a certain flexibility for interpretation during correlation is required; issues have arisen when discussing with other geologists, who sustain that the final number of resulting formal lithostratigraphic units is extremely high, too local, and the resulting legend integrating all types of stratigraphic units gets saturated. This problem could be solved by considering the main unconformity-bounded units or lithosomes as representative of the fundamental stages of evolution of DJVC, thus providing a tool for stratigraphic synthesis.

The stratigraphy of the DJVC is framed between four (4), second-order unconformities (D1-4), which correspond to the angular contact-surfaces given by the borders of the vt, sc1, vc1, and vc2 volcano-tectonic structures. Such surfaces mark the successive destruction of each edifice, implying critical changes in the volcano-magmatic system. With the distance, unconformities are represented by thick, secondary volcaniclastic sequences, suggesting significant mass-wasting periods, and by epiclastic deposits, and paleosol bedsets. The identification of the second-order unconformities allowed the definition of five (5) synthems, which comprise deposits of lava-domes, lava-flows, pyroclastic density currents (including all spectra within those generated by column collapse and those produced by lava-dome collapse), lahars, and debris-avalanches, with interbedded external lithosomes originated at the neighbouring Las Ánimas volcano. This stratigraphic framework provides information on the eruptive history of DJVC, which comprises the following lithosomes, in chronological order: (1) remnants of a primordial, <1.5±01 Ma, effusive edifice (Santa Helena), truncated at its summit by a SW-NE trending, morphotectonic depression (vt=D1); (2) remnants of an adventice cone (pre-Montoso), with it's western flank truncated by a sector-collapse scar (sc1= D2), from which a debris-avalanche deposit was originated; (3) remnants of a stratocone (Ancestral

Doña Juana), truncated at its summit by a 3-km caldera structure (vc1= D3), associated to a ~40 030 ± 560 yr BP ignimbrite; (4) remnants of a second stratocone (Old Doña Juana), truncated at its summit by a ~2,8 km caldera structure (vc2= D4), correlated to variably-welded ignimbrites; (5) an adventice cone (Montoso), truncated to the W by a sector-collapse scar (sc1= d4a) ; and (6) three dacitic, lava-dome fields: El Filo (ld3) and Totoral (ld4) dome-fields grew up along the previous caldera borders, whereas the Doña Juana dome-field (ld5), correspond to intracaldera lava-domes (Fig.1). The latest volcanic activity of DJVC has been characterised by the construction and partial destruction of the Doña Juana lava-dome field, which has resulted in block-and-ash flows, surges, and lahars, dated at 990 ±30 yr BP (1120-1090 AD), 320 ±30 yr BP (1650-1470 AD), 610 ±30 yr BP (1410-1290 AD), and 105 ±42 yr BP (1800-1940 AD); the latter corresponds to the events documented in historical records, from 1897 to 1906 AD, reflecting a substantial volcanic hazard for the populated areas surrounding the DJVC.

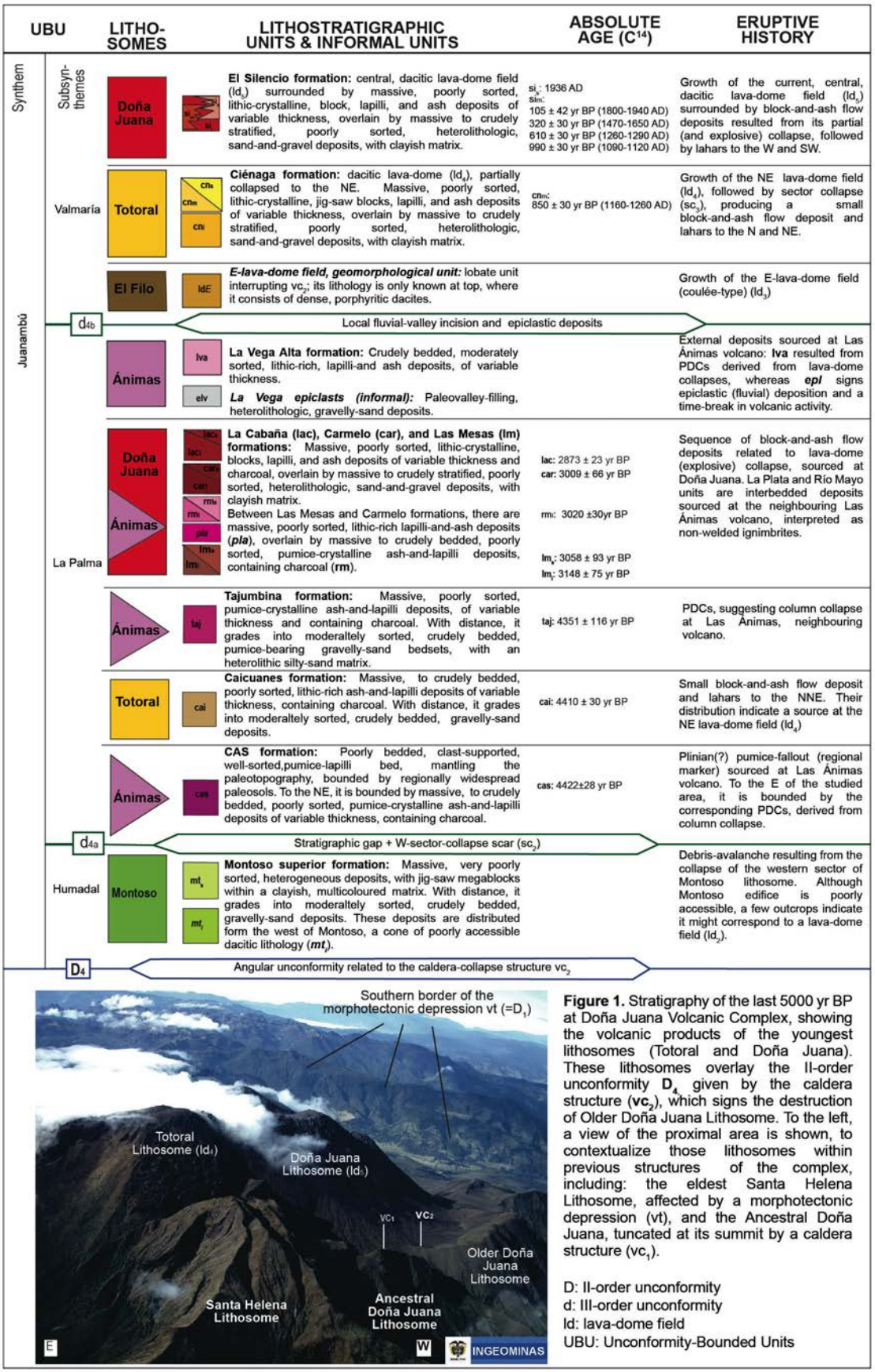

Figure 1. Stratigraphy of the last 5000 yr BP at Doña Juana Volcanic Complex, showing the volcanic products of the youngest lithosomes (Totoral and Doña Juana). These lithosomes overlay the II-order unconformity **D_4** given by the caldera structure (**vc_2**), which signs the destruction of Older Doña Juana Lithosome. To the left, a view of the proximal area is shown, to contextualize those lithosomes within previous structures of the complex, including: the eldest Santa Helena Lithosome, affected by a morphotectonic depression (vt), and the Ancestral Doña Juana, tuncated at its summit by a caldera structure (vc_1).

D: II-order unconformity
d: III-order unconformity
ld: lava-dome field
UBU: Unconformity-Bounded Units

The lobe-hyaloclastite in the Madneuli deposit: useful criteria for the reconstruction of a lava dome structure, Lesser Caucasus, Georgia

Nino Popkhadze[1], Robert Moritz[2]

[1] A.Janelidze Institute of Geology of Iv.Javakhisgvili Tbilisi State University, (nino_popkhadze@yahoo.com); [2] Department of Earth Sciences, University of Geneva, Switzerland.

The Bolnisi district is part of a major late Cretaceous volcano-sedimentary belt belonging to the Tethyan orogenic and metallogenic belt (Mortiz et al., Richards eds.) Towards the east, along the Black Sea, this belt is known as the Eastern Pontides in Eastern Turkey. According to the majority of previous studies, the formation of the Madneuli deposit is tightly linked to the evolution of late Cretaceous magmatism in the Bolnisi district, where volcanism has a bimodal character.

The host rocks of the Madneuli deposit consist of felsic volcanic and volcano-sedimentary rocks of rhyodacitic composition. Twelve lithofacies were singled out in our study for the first time at the Madneuli deposit. Lithofacies units, described within the host-rock succession of the Madneuli deposit, are grouped in two facies assemblages: a stratigraphically lower volcanogenic sedimentary facies assemblage and an upper volcanic facies (Popkhadze et al., 2013). In the Madneuli open pit, it is possible to observe fragments of lobe-Hyaloclastite flow: massive, coherent lava, flow-banded border zone of lava, carapace breccia, individual lobes and two types of hyaloclastite: hyaloclastite with glass-like selvages and with pillow-like forms (Popkhadze et al., 2012; 2014), (Fig.1).

The internal and a few isolated lobes together create the dome structure in the open pit. In the southeastern part, there is a ring structure of isolated lobes within the massive facies with internal columnar joints, which resembles glass-like selvages of the Hyaloclastite of its distal part. Hyaloclastite with glass-like selvages refers to a breccia facies, morphologically associated with carapace breccias occurring along the upper surface of the distal part of the flows. By contrast, hyaloclastite with pillow-like forms is pumiceous hyaloclastite, which consists of pumice fragments and volcanic glass. The structures of pumiceous Hyaloclastite differ from Hyaloclastite with glass-like selvages, as they are the products of different lobes, formed by different pulses of lava at the periphery of the lava dome. It is also possible to observe fragments of carapace breccia in the eastern uppermost part of the open pit, and has a local, limited distribution. The Hyaloclastite is poorly sorted and crudely layered. It consists of lobe fragments, massive and flow banded, set in a Hyaloclastite matrix (Gibson et al., 1998). The petrographic description shows a different nature: hyaloclastite with glass-like selvages are characterized by devitrification of volcanic glass, which is replaced by quartz and K-feldspar overgrowths in the groundmass and elongated K-feldspar phenocrysts. Classical perlitic cracks were identified during thin section observation.

The hyaloclastite with pillow-like forms consists of relics of volcanic glass and large pumice clasts replaced by sericite. The hyaloclastite types described in the Madneuli open pit are associated with submarine dome-like structures of felsic magmas and they were emplaced during several pulses

(or eruptions). During the earliest pulses, lava was directly extruded in the volcanogenic sedimentary bedded unconsolidated rocks. The lower part of these rocks is the products of phreatomagmatic explosion, which is strongly silicified, and is ore bearing. The upper part is mostly represented by turbiditic rocks and bedded volcanogenic sedimentary rocks. The clear evidence of this are slumps in the bedded rocks, the fragments of glass-like selvage hyaloclastite were found in breccia within this bedded volcanogenic sedimentary facies assemblage. Also numerous folds and fractures were developed, some of them being associated with uplift during the formation of the dome structure. The newly rising magma may have intruded along these faults or fractures and invaded previously emplaced, but still water-saturated glass-like selvage hyaloclastite. There are no constraints on the exact water depth during formation of hyaloclastite. The presence of pumiceous rhyodacitic hyaloclastite implies that volatile exsolution was not inhibited by pressure (Yamagishi et al., 1985), which indicates that water depth was shallow, probably less than 300-200 m. The products of preatomagmatic eruption, represented by vesiculated fine-grained tuff, associated with accretionary lapilli horizons, indicate that the eruption was distant by several kilometers from the Madneuli deposit. It is possible, that this effects of magma chamber to arise the eruption in the open pit.

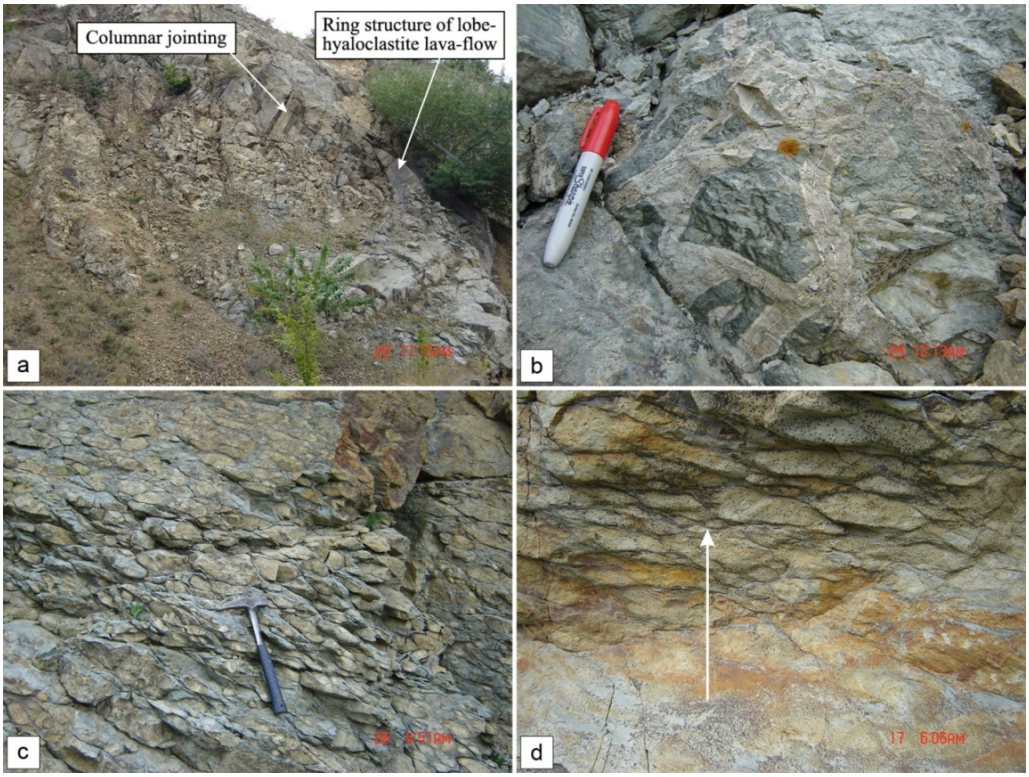

Fig. 1 - *Representative examples of hyaloclastite outcrops at Madneuli: a - Margins of a lobe hyaloclastite flow with internal columnar joints. b - Carapace breccia. c - Pillow-like shapes in hyaloclastite. d - Transitional zone from massive to pillow-structured parts in pillow-like hyaloclastite.*

References

Gibson H., Morton R., Hudak G. (1998). Submarine volcanic processes, deposits and environment favorable for the location of volcanic-associated massive sulfide deposits. Reviews in Economic Geology, 8, 13-51.

Yamagishi H., Dimroth E. (1985). A composition of Miocene and Archean rhyolite hyaloclastites: evidence for hot fluid rhyolite lava. Journal of Volcanology and Geothermal Research, 23, 337-355.

Moritz R., Melkonyan R., Selby D., Popkhadze N., Gugushvili V., Tayan R., and Ramazanov V. Metallogeny of the Lesser Caucasus: From arc construction to post-collision evolution. In: Jeremy Richards et al. (eds), Tethyan metallogeny, Special Publication of the Society of Economic Geology, in press.

Popkhadze N., Moritz R., Gialli S., Beridze T., Gugushvili V., Khutsishvili S. (2013). Major volcano-sedimentary facies types of the Madneuli polymetallic deposit, Bolnisi district, Georgia: Implications for the host rock depositional environment. In: Erik Jonsson et al. (eds), Mineral deposit research for a high-tech world, 12th SGA Meeting, Sweden, Uppsala, 2, 576-579.

Popkhadze N. (2012). First evidence of hyaloclastites at Madneuli deposit, Bolnisi district, Georgia. Bulletin of the Georgia National Academy of Sciences, 6, 83-90.

Popkhadze N., Moritz R., Gugushvili V. (2014). Architecture of Upper Cretaceous rhyodacitic Hyaloclastite at the polymetallic Madneuli deposit, Lesser Caucasus, Georgia. Central European Journal of Geosciences, 6, 308-329.

Stratigraphy of Sierra de Chauchaiñeu, Patagonia, Argentina

Flavia M. Salani & Marcela B. Remesal

IGEBA- Consejo Nacional de Investigaciones Científicas y Técnicas-FCEN, Universidad de Buenos Aires, Argentina, (*flaviamsalani@gmail.com).

The Cenozoic of north central argentine Patagonia is characterized by Oligocene and Miocene extensive volcanism. During the Miocene the eruptive activity built several polygenic volcanic complexes, which constitute the main structure of different sierras. One of the most voluminous sequences crops out at Sierra de Chauchaiñeu (1800 masl, 68º 30´and 68º 05´ WL; 41º 40´ and 42º 05´ SL) and is referred to as Barril Niyeu Volcanic Complex (BNVC) in reference to the homonymous place located in the northern foothills of this range.

The Barril Niyeu Volcanic Complex (Fig.1) comprises a basaltic-trachyte lithological association of both effusive and explosive activity (lava flows, lava domes, ash fall, pyroclastic flows, breccias and clastogenic lavas).Methodology: Prior to fieldwork, an interpretation of the area was made from satellite images in order to identify the main volcanic units and in particular the eruptive vents. Mapping was performed on the bases of transects in addition to local surveys, and in some cases geochronological determinations assistance was essential to the definition of units. According to the observed distribution and volcanic stratigraphy, six volcanic units could be recognized (Fig. 1).

Alkaline basalts: Are located at the base of the basaltic sequence, cropping out East of Buitrera caldera and at the SW area. The vents have not been identified. The lavas are mostly porphyritic composed by iddingsitized olivine, Ti-augite and plagioclase (An50-52). Some basalts have brecciated texture or show clastogenic features revealing the explosive nature of the eruptions, and producing strombolian deposits. Trachyte lava flows: The earliest eruptive stage (K/Ar, 20.6±0.4 Ma) of the BNVC produced viscous trachyte lava restricted to the volcanic center. Trachyte rocks mostly occur as thick lava flows and constitute the core of the sierra de Chauchaiñeu. They show columnar or flabelliform jointing, fluidality and vesiculation features. The maximun thickness is 100m. The lavas are porphyric, with sanidine and aegirine, aegirine/augite phenocrysts set in a trachytic groundmass. Pyroclastic Unit 1: This late pyroclastic stage has dominant intermediate to acid composition produced air-fall, mainly plinian (lesser strombolian) and pyroclastic flow deposits. Pyroclastic flows have different thickness ranging from 20 to 70 m, in the Pilquiniyeu area.

In Barranca de los Loros they show minor expressions (1-2 m) and occurr interlayered with air fall lapilli deposits. They are composed mainly by vitroclasts, (10-15%) volcanic lithics (basalts and trachytes), and scarse crystals. Locally strombolian deposits, lapillite and agglomerate are distinguished. Sometimes these deposits are interlayered with trachyte and basaltic flows. Pyroclastic Unit 2: The later pyroclastic stage is characterized dominantly by ignimbrites that commonly overlay trachyte lavas and, to a smaller extent, the older pyroclastics flows. Rocks are

composed of crystals (30-20%) of sanidine, embayed quartz, with subordinated zircon and opaque minerals; lithic fragments (<10%) of trachyte and basaltic volcanics. Vitroclastic components are pumice and devitrified glass shards. Trydimite occurs as vapour phase crystallization. The deposits show different welding degrees which, in many cases, produce eutaxitic textures. Strombolian deposits are lapilli and block size, mainly composed of brown glassy patches, porfiritic pumices with olivine crystals, and basaltic lithic fragments. Trachybasalt flows: The last eruptive stage of the BNVC corresponds to the trachybasalts (K/Ar, 18.7±0.4Ma) which appear either as lava flows or as spatter cones. The lava flows form a sequence plateau like whose most important development is seen to the north of the Sierra de Chauchaiñeu. All these rocks are basalts slightly porphyritic, mainly composed of plagioclase microlites arranged with flow texture, crystals of titaniferous augite, olivine, generally better developed than pyroxene, in many cases with skeletal crystals and alterated to iddingsite. Lava domes: The lava domes within the four cauldrons of the complex are composed either of comendites or quartz-trachytes. Comendites are aphyric with seriated texture constituted by feldspar, amphibole and trydimite. Petrography of quartz-trachytes is defined by phenocrysts of quartz and sanidine, set in a glassy and devitrified groundmass with arfvedsonite as mafic component, titanite and zircon.

Evolution of Barril Niyeu volcanic Complex: While various stages are recognized in the effusiveness of the complex, in some cases there is simultaneity of events of different compositions. An early episode of porphyric basaltic lavas begins the construction of the BNVC and it was succeeded by trachytic lavas outpouring, accompanied by pyroclastic rocks (first pyroclastic episode). A second pyroclastic episode of dominantly ignimbritic character and the site of acidic /mesosilicic domes constitute the proximal sectors of this volcanic structure. The evolution is completed with the issuance of new basic lava facies that shape the distal areas of the Volcanic Complex.

Volcanic structure: This large volcanic construction was built through several stages of eruptive activity outpoured from at least five emission centres of distinct trachyte/rhyolite and basaltic compositions. The CVBN is the product of a complex structure with a main emission vent, Chauchaiñeu Caldera, approximately circular of 5 km of larger diameter. Associated to this structure are trachyte lavas, ignimbrites and basaltic flows; and four comenditic, irregularly shaped, domes with maximum size of 1 km of major axis. Two smaller calderas (Caldera Buitrera Buitrera North and South), occur very close together, about 1.7 km and 2.5 km in diameter, in the eastern sector. In the southeast area a center of 3.8 km in diameter is defined by diverging pyroclastic and lava emissions. The latter was recently nominated Caldera Talagapa Chico. Both South Buitrera Caldera as Talagapa Chico have trachyte bodies inside. In the western part, it is distinguished Choique Corral Caldera, a circular structure whose limits are marked by trachyte lava flows radiating mostly to the west; the eastern rim is less visible, since it is partly hidden by a trachyte lava flow outpoured from the main center (Chauchaiñeu Caldera).

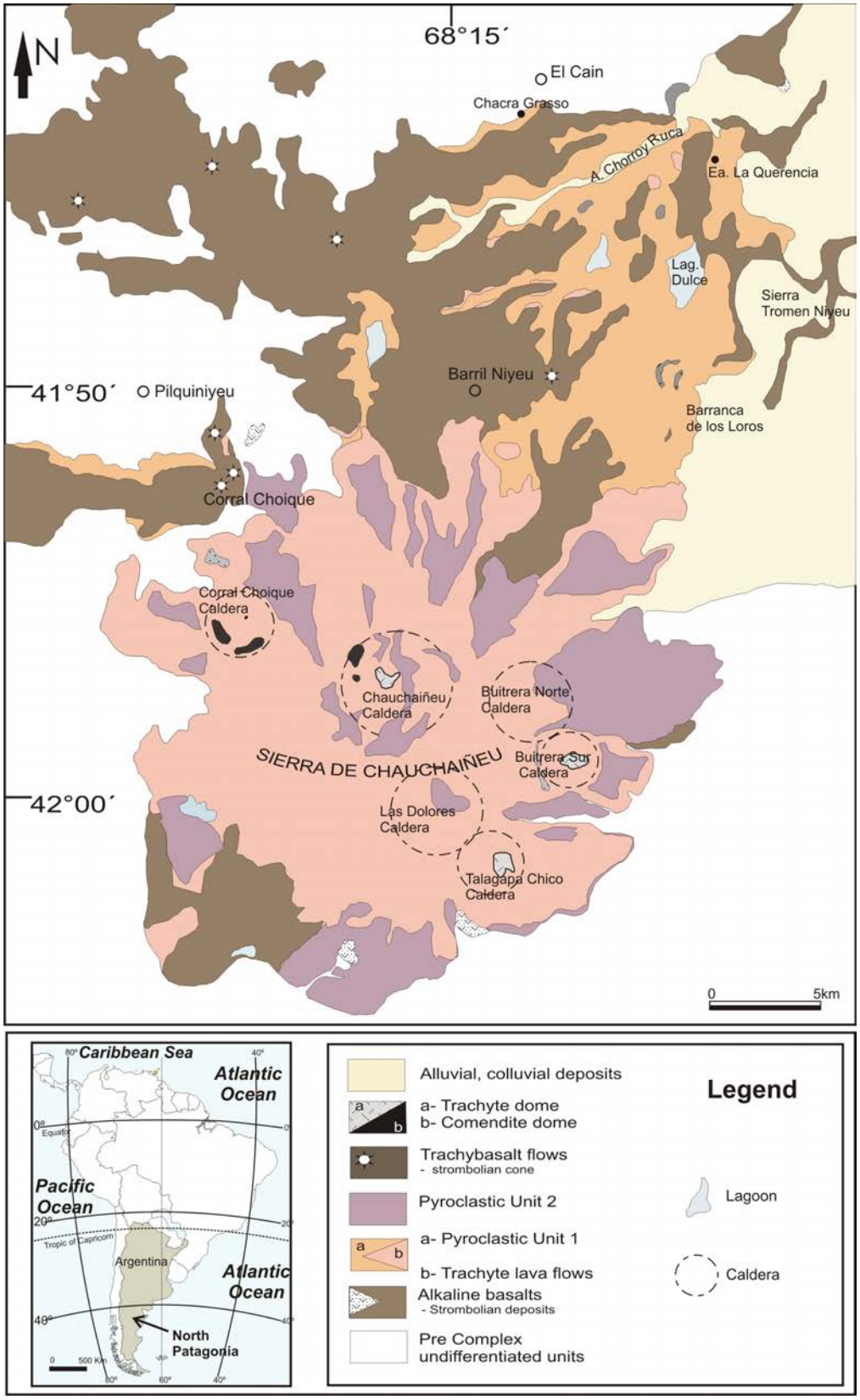

Fig.1 - *Geological map of Barril Niyeu Volcanic Complex.*

Stratigraphy and volcanology of Procida Island (Campi Flegrei, Italy)

Claudio Scarpati, Annamaria Perrotta, Vincenzo Morra

Dipartimento di Scienze della Terra, dell'Ambiente e delle Risorse. Università di Napoli Federico II, largo San Marcellino 10, 80138 Napoli, Italy, (claudio.scarpati@unina.it).

An up-to-date stratigraphic reconstruction of Procida Island is hereby presented together with a new geological map. The geological field survey was carried out at a 1:5000 scale. Furthermore, a detailed stratigraphic analysis, at a 1:10 scale, of several measured vertical sections was performed. The complex volcanic history of this area is characterized by the superposition of minor effusive, main explosive, and some reworked volcanic products. The stratigraphic relationships between autochthonous volcanic products and pyroclastic products erupted from different source areas (e.g., Ischia Island) are taken into account. The proposed stratigraphy is based on the integrated use of stratigraphic and eruptive units, which can coincide or, more frequently, have different hierarchy. The main stratigraphic criterion in the field survey was the identification of eruptive units that represent the product of single eruptions. Eruptive units are defined as a deposit or succession of deposits bounded by paleosols or erosional surfaces indicating a significant break in the volcanic activity. Each eruptive unit will be described on the basis of its structural and textural properties and lithology. Paleosols are adopted as stratigraphic markers of quiescence periods. Eruptive units are grouped into lithostratigraphic bodies shown on the geological map. In this way, a single formational unit is composed of one or more eruptive units. We use lithosomes as informal stratigraphic units in order to put in evidence volcanic centers that are still morphologically recognizable. In the Campi Flegrei volcanic field, these volcanic centers are monogenic. The stratigraphy of Procida Island provides a useful synthesis of the volcanological evolution of this area. The recognized units include successions that represent all the main eruptive phases of Campi Flegrei. Despite the large number of recognized eruptive units and the lack of geochronological constraints for most of them, the volcanic activity is concentrated in relatively short time periods. Subaerial and marine erosion that dissected and reworked a large part of the volcanic successions occurred during longer quiescent periods. The onset of volcanic activity in this area is represented by products related to the activity of scattered vents of unconstrained age. From 74 to 55 ka, they were mantled by products erupted in the nearby island of Ischia. Circa 39 ka, the Campanian Ignimbrite eruption occurred in the Campi Flegrei area, producing a large caldera. A thick succession of welded pyroclasts, lithic breccias, and associated ash- and pumice-flow deposits was emplaced in the proximal area. The local activity resumed at 19 – 17 ka with the formation of monogenetic volcanoes. A phreatoplinian eruption (Neapolitan Yellow Tuff) occurred at 15 ka, which produced a second, nested caldera. Minor tephra layers testify to the final explosive activity vented in this area.

India's volcanic frontier: Andaman volcanoes

Hetu Sheth

Department of Earth Sciences, Indian Institute of Technology Bombay, Powai, Mumbai 400076 India, (hcsheth@iitb.ac.in).

Though the Indian subcontinent experienced extensive volcanism in the geological past (such as the famous Deccan Traps), India's only active volcano today, named Barren Island, is in the Andaman Sea. Another Indian volcano named Narcondam, 120 km NNE of Barren Island, is dormant. Barren Island is thus the northernmost active volcano of the great Indonesia-Andaman subduction zone. The regional tectonic setting is complex, including subduction (of the Indian Plate under the Eurasian Plate), major right-lateral transform faulting and formation of a "sliver" plate (the Burmese Plate), and back-arc spreading in the Andaman Sea since 4 Ma.

Barren Island (standing ~350 meters above sea level and >2 km above the sea floor) had explosive eruptions (producing tuff breccias, scoria and ash beds) and effusive eruptions (producing 'a'ā lava flows), followed by caldera formation, in prehistoric time (Sheth et al., 2009). The oldest subaerial lava flows on the island are dated at 1.58 ± 0.04 Ma (2σ) (Ray et al., 2015). Ash layers from the volcano thousands of years old, some containing plagioclase lithic crystals 1.8 Ma in age, have been identified in sediment cores from the Andaman Sea (Awasthi et al. 2010; Ray et al., 2013).

A scoria cone born within Barren Island's caldera marks volcanic resurgence and was active periodically from 1787 to 1832 (the historic eruptions). Since 1991, the same scoria cone has produced six eruptions, many with lava flows, including a flow with squeeze-ups of highly crystalline and viscous toothpaste lava (Sheth et al., 2011). All Barren Island rocks are highly porphyritic basalt and basaltic andesite, with only rare andesite in the prehistoric sequence. They show incompatible element signatures typical of subduction zone magmas, but have some of the most "depleted" (mantle-like) radiogenic isotopic signatures (Sr-Nd-Pb). In comparison, Narcondam (710 meters above sea level) is dominated by highly porphyritic andesite and dacite, sometimes containing mafic enclaves (indicating mafic recharge and magma mingling) and showing assimilation of continental crustal material (in e.g., quartz xenocrysts and isotopic ratios) (Luhr and Haldar 2006; Pal et al., 2007; Streck et al., 2011). Links to Barren Island's eruptions to giant earthquakes, such as the 26 December 2004 Great Sumatra megathrust earthquake, have been claimed.

An analysis of the earthquake records for the region and the eruption records of Barren Island (and Talang volcano in Sumatra) shows no correlation between large earthquakes and volcanic eruptions (Sheth 2014). The polygenetic scoria cone of Barren Island (at least 13 eruptions since 1787), named Shanku ("cone"), has two excellent analogues, namely Anak Krakatau in Indonesia (40 eruptions since 1927), and Cerro Negro in Nicaragua (23 eruptions since 1850). Some remarkable similarities exist between these three volcanoes (in magmatic processes, compositions, eruption styles). Shanku's ≥227-year-long activity is driven by purely magmatic processes, without external

triggers (earthquakes). Calculations show that feeder dykes ~0.5 m thick and a few hundred meters long, originating from shallow-level magma chambers (~5 km), are suitable for the Shanku eruptions (Sheth 2014). Polygenetic scoria cones like Shanku, Anak Krakatau and Cerro Negro may be commoner than generally perceived, and this category of volcanoes, in between classical small-volume "monogenetic" scoria cones and certified, larger "polygenetic" volcanoes, deserves recognition and importance. Volcanoes that are highly active, close to large human populations, yet poorly dated, and unmonitored, are significant hazards. Barren Island is all of the above, with six significant eruptions between 1991 and 2014, the last one ongoing. It is ~500 km from the Myanmar and Thailand coasts, 135 km from the Andaman Islands' capital Port Blair, and a mere 80 km from Middle Andaman Islands, all regions with dense populations. The volcano is also located on a very busy sea and air traffic route between south and southeast Asia. Narcondam, dormant now, may have erupted in the Holocene and is potentially active (Siebert et al., 2010). Even if dormant (or extinct), it poses significant hazards in the form of volcano collapses and possible tsunamis, which may have occurred in the past, as suggested by its topographic features. Unfortunately, though the earthquake hazard in the Andaman region has received much attention (especially after the December 2004 Sumatra megaearthquake) and the region is being extensively studied by geophysicists, the volcanic hazard still receives little attention.

References

Awasthi N., Ray JS., Laskar AH., Kumar A., Sudhakar M., Bhutani R., Sheth HC., Yadava MG. (2010). Major ash eruptions of Barren Island volcano (Andaman Sea) during the past 72 kyr: clues from a sediment core record. Bullettin of Volcanology, 72:1131-1136.

Luhr JF. and Haldar D. (2006). Barren Island volcano (NE Indian Ocean): island-arc high-alumina basalts produced by troctolite contamination. Journal of Volcanology and Geothermal Research, 149:177-212.

Pal T., Mitra SK., Sengupta S., Katari A., Bandopadhyay PC., Bhattacharya AK. (2007). Dacite-andesites of Narcondam volcano in the Andaman Sea – an imprint of magma mixing in the inner arc of the Andaman-Java subduction system. Journal of Volcanology and Geothermal Research, 168:93-113.

Ray JS., Pande K., Awasthi N. (2013). A minimum age for the active Barren Island volcano, Andaman Sea. Current Science, 104:934-939.

Ray JS,. Pande K., Bhutani R. (2015). 40Ar/39Ar geochronology of subaerial lava flows of Barren Island volcano and the deep crust beneath the Andaman island arc, Burma microplate. Bullettin of Volcanology, 77:57 - 10.1007/s00445-015-0944-9.

Sheth HC. (2014). What drives centuries-long polygenetic scoria cone activity at Barren Island volcano? Journal of Volcanology and Geothermal Research, 289-64-80.

Sheth HC., Ray JS., Bhutani R., Kumar A., Smitha RS. (2009). Volcanology and eruptive styles of Barren Island: an active mafic stratovolcano in the Andaman Sea, NE Indian Ocean. Bullettin of Volcanology, 71:1021-1039.

Sheth HC., Ray JS., Kumar A., Bhutani R., Awasthi N. (2011).Toothpaste lava from the Barren Island volcano (Andaman Sea). Journal of Volcanology and Geothermal Research, 202:73-82.

Siebert L., Simkin T., Kimberly P. (2010). Volcanoes of the World. 3rd Edn. Smithsonian Institute and University of California Press, USA, 551.

Streck MJ., Ramos F., Gillam A., Haldar D., Duncan RA. (2011). The intra-oceanic Barren Island and Narcondam arc volcanoes, Andaman Sea: implications for subduction inputs and crustal overprint of a depleted mantle source. In: Ray J, Sen G, Ghosh B (eds) Topics in igneous petrology. Springer, 241-273.

Petrology of La Primavera caldera magmas; the Tala Tuff case study.

Giovanni Sosa Ceballos[1], José Luis Macías Vázquez[1], Diego Miguel Cruz[2]

[1] Instituto de Geofísica, Unidad Michoacán, UNAM; [2] Facultad de Ingeniería, UNAM.

La Primavera caldera, Jalisco Mexico, is a Pleistocenic volcanic structure formed by dome complexes and multiple pyroclastic flows and fall deposits. It is located at the intersection of the Chapala, Colima, and Tepic grabens in western Mexico. The caldera collapse occurred 95 ka and is associated to the eruption of ~20 km^3 of pumice flows known as the Tala tuff (Mahood 1980).

In order to better understand the plumbing system that tapped the Tala tuff and to investigate its relation with the geothermal field at La Primavera we performed a series of hydrothermal experiments and studied melt inclusions hosted in quartz phenocrysts by Fourier Infra red stectroscopy (FTIR).

The Tala tuff is formed by two groups of pumice with different mineral content (one contain fayalite and ferrohedenbergite), very low cristallinity (<3%) and low vesicularity but exactly same bulk composition. We ran NNO and QFM buffered experiments. QFM experiments does not crystallized neither fayalite, nor ferrohedenbergite. The absence of titanomagnetite does not allowed us to calculate pre-eruptive temperatura by the Fe-Ti oxides method. However, the stability of quartz and plagioclase, which are natural phases, suggest that temperature should be less than 750 °C at a pressure of 200 MPa. In addition we ran Rhyolite-Melts simulations and confirm < 800 °C temperaturas. The analyses of H_2O and CO_2 dissolved in melt inclusions yielded concentrations of 2-5 wt.% and 50-100 ppm respectively. This data confirm that the pre-eruptive pressure of the Tala tuff is ~200 MPa and in addition to major elements compositions suggest that the Tala tuff is either, compositionally zoned or mixed with other magma just prior to eruption.

Postglacial eruptive history of Barrancas Center, Laguna del Maule Volcanic Complex (36° 10´S, 70° 30' W), Chile

Patricia Sruoga[1], Manuela Elissondo[2]

[1]CONICET-SEGEMAR, Buenos Aires, Argentina, (patysruoga@gmail.com); [2]SEGEMAR, Buenos Aires, Argentina (manuelaje@yahoo.com.ar).

The Laguna del Maule Volcanic Complex (LMVC) is among the most active Pleistocene-Holocene rhyolitic centers globally. It covers ~ 500 km^2 on the Argentina-Chile border in the Southern Volcanic Zone. At least 130 separate vents erupted > 350 km^3 of effusive and explosive products since 1.5 Ma, suggesting persistence of a large magma reservoir (Hildreth et al., 2010). These include 24 postglacial vents which encompasses rhyolite and rhyodacite lava flows and domes, accompanied by tephra falls and pyroclastic flows. This recent flare-up of silicic volcanism has yielded at least 50 rhyolitic eruptions in the last 26 ka (Singer et al., 2014). Soil ^{14}C dating and chemical correlation suggest that at least 33 mostly silicic lavas and pyroclastic units from LMVC vents are younger than 14 ka with half of them younger than 3.5 ka (Fierstein et al., 2014). Several geophysical studies document ongoing volcanic unrest within the LMVC. Geodetic observations since 2007 by both continuous GPS and InSAR have recorded uplift at a rate in excess of 20 cm/yr (Fournier et al., 2010; Feigl et al., 2014; Le Mével et al., 2015). In addition, frequent seismic swarms have been occurring at shallow depths at south LMVC (SERNAGEOMIN-OVDAS, unpublished REPORTS 20112-2015). Preliminary gravity, magnetotelluric and conductivity results also suggest the presence of a shallow magma system beneath the same area of deformation (Singer et al., 2014).

Barrancas center, located at the southeastern LMVC, represents the most highly-productive and longest-lived postglacial vent. Due to the geophysical-documented ongoing unrest, unraveling its eruptive history is a key task in hazard-oriented assessment. Since 2011, detailed mapping has been carried out in the framework of an international collaboration project (SEGEMAR, SERNAGEOMIN, USGS, University of Wisconsin). Our main goal is to obtain a high-quality hazard map, based on precise identification of the products and accurate reconstruction of the eruptive stratigraphy. The ~5.5 km^3 postglacial volcanic record is mainly preserved in Argentina, at the headwaters of Barrancas river (Sruoga et al. 2015) (Fig. 1). Two stages may be distinguished: 1) an early episode of dome building is dated at ~14.5 ka (Andersen et al., unpublished) and is followed by an explosive dome partial-collapse event that produced widespread block and ash deposits, up to ~60 m thick, extending ~13 km from source along Curamilio, Puente de Tierra and La Parva creeks (Fig. 1) and 2) 8 obsidian flows (Hildreth et al., 2010) and 3 pumice cones which produced highly –recurrent tephra falls and several pyroclastic flows. One of the lava flows has been dated at 6.4 ka (Singer et al. 2014). The pyroclastic sequence Pampa del Rayo includes not only the explosive record of Barrancas center, but also of other synchronic LMVC vents.

Ongoing tephrocronology studies and Ar/Ar dating will undoubtedly improve our understanding of a volcano which in case of reactivation may affect a widespread area in Chile and Argentina, particularly in south Mendoza and North Neuquen.

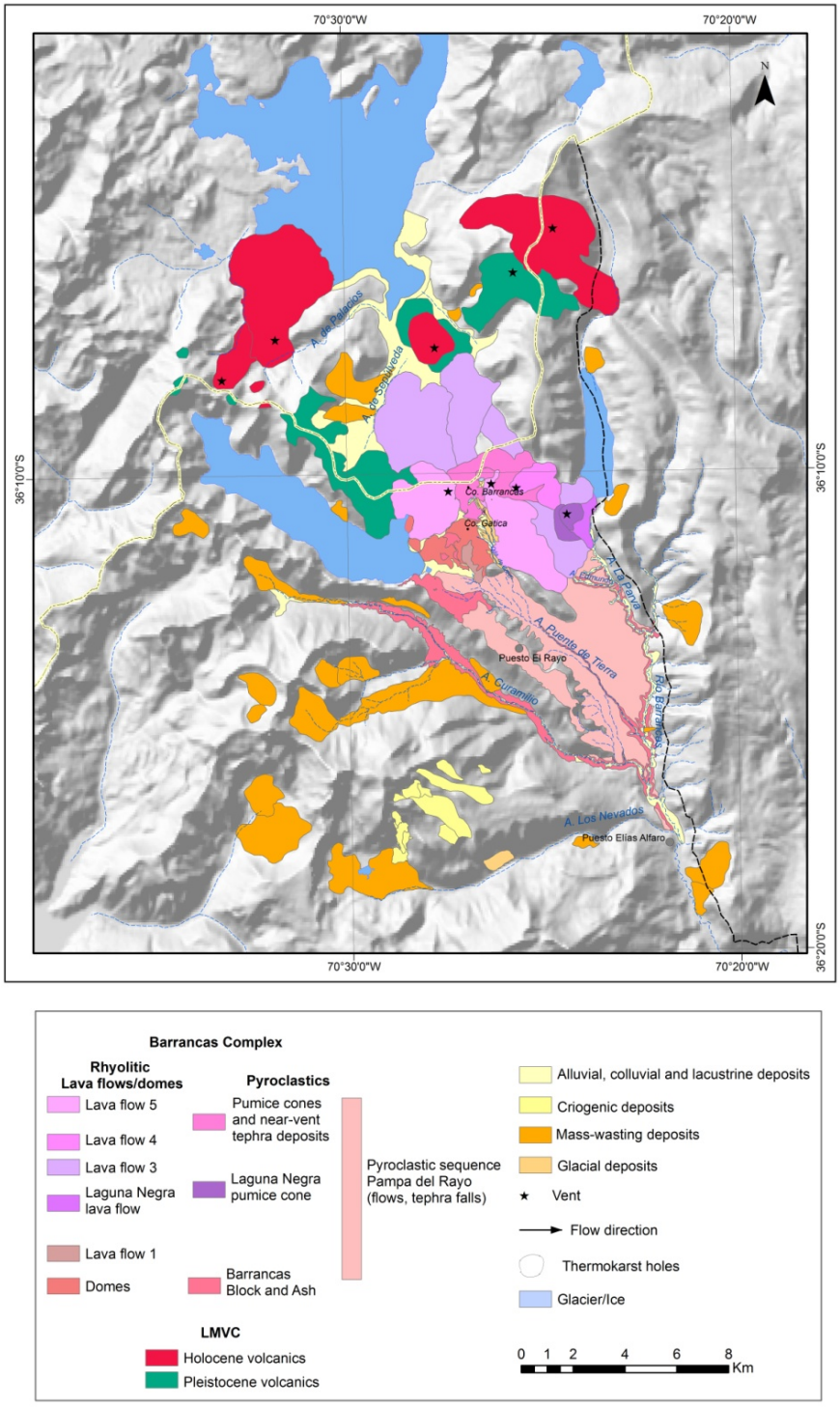

Fig. 1 - *Geologic map of Barrancas center.*

References

Hildreth W., Godo E., Fierstein J., Singer B. (2010). Laguna del Maule Volcanic Field. Eruptive history of Quaternary basalt-to-rhyolite distributed volcanic field on the Andean rangecrest in Central Chile. Subdirección Nacional de Geología SERNAGEOMIN. Boletín 63, 144.

Feigl K.L., Le Mével H., Tabrez Ali S., Córdova L., Andersen N.L., DeMets C., and Singer B.S. (2014). Rapid uplift in Laguna del Maule volcanic field of the Andean southern volcanic zone (Chile) 2007-2012: Geophysical Journal International 196, 885–901, doi: 10.1093/gji/ggt438.

Fierstein J., Sruoga P., Amigo A., Elissondo M., Rosas M. (2014). Tephra in Argentina establishes postglacial eruptive history of Laguna del Maule volcanic field in Chile: 36 silicic eruptions in 14,000 years.

Fournier T.J., Pritchard M.E., Riddick S.N. (2010). Duration, magnitude, and frequency of subaerial volcano deformation events: New results from Latin America using InSAR and global synthesis. Geochemistry Geophysics, Geosystems 11(29).

Le Mével H., Feigl K.L., Córdova L., Demets C., and Lundgren P. (2015). Evolution of unrest at Laguna del Maule volcanic field (Chile) from InSAR and GPS measurements, 2003 to 2014: Geophysical Research Letters 42, 6590–6598, doi: 10.1002/2015GL064665.

Singer, B.S., Andersen N.L., Le Mével H., Feigl K.F., DeMets C., Tikoff B., Thurber C.H., Jicha B.R., Cardona, C., Cordoba M., Gil F., Unsworth M.J., Williams-Jones G., Miller C., Hildreth W., Fierstein J., Vazquez J. (2014). Dynamics of a large, restless, rhyolitic magma system at Laguna del Maule, southern Andes, Chile. Geological Society of America Today 24, 4-10.

Sruoga P., Elissondo M., Fierstein J., García S., González R., Rosas M. (2015). Actividad explosiva postglacial del centro Barrancas, Complejo Volcánico Laguna del Maule (36° 05' S, 70° 30' O). Peligrosidad en Argentina. XIV Congreso Geológico Chileno, Actas At4St11 013. La Serena.

Multiple Approaches to Interpreting Volcano Stratigraphy in New Zealand: a Synthesis

Bob Stewart & Károly Németh

Volcanic Risk Solutions, Soil & Earth Sciences, Institute of Agriculture and Environment, Massey University, Palmerston North, New Zealand, (R.B.Stewart@massey.ac.nz).

Interpreting New Zealand volcanoes has involved multiple approaches throughout the history of volcanological investigations of those volcanoes. A comprehensive tephrostratigraphy of rhyolite eruptions from central North Island was first developed by Vucetich and Pullar (1964), who recognized the importance of tephra identification to the interpretation of soil patterns and processes. This involved painstaking exposure by exposure mapping and correlation across the central North Island with age control provided by ^{14}C dating. This pioneering work provided the tephrochronological framework for the more detailed studies that followed. Climate influences have also been widely recognized as providing markers in the stratigraphic record. On a broad scale, marine terraces formed by sea level high stands on the Taranaki Coast (Pillans 1990), as a result of stadial-interstadial and glacial-interglacial fluctuations, have been used to constrain the ages of volcanic events, such as large-scale debris avalanches in Taranaki (Alloway et al., 2005). Over shorter timescales, change in sedimentary regime from volcanic loess to medial ash deposition at the end of the last glaciation provides a stratigraphic marker across the North island of New Zealand, along with paleoclimate-related paleosol development (Stewart, et al, 1977; Newnham et al 2003). Variations in aerosolic quartz accumulation in quartz-free andesitic ash sequences have been used to correlate terrestrial tephra-dominated sequences to oxygen isotopes stages (Stewart, et al,1977; Alloway et al., 1992), providing a somewhat unusual timescale for terrestrial volcanic processes. Increased sedimentation resulting from erosion associated with accelerated lahar and debris avalanche activity has also been correlated with cold periods (Zernack et al., 2009, 2012; Tost, et al., 2015). One of the key advantages for interpreting NZ andesite volcanic sequences is the presence of rhyolitic tephras from the Taupo Volcanic Zone which have been well dated (Froggat and Lowe, 1990, Lowe et al., 2008), together with discrimination using glass chemistry (Stokes at al 1992). This provides a stratigraphic framework for constructing 3-D models of volcano architecture for the andesite stratovolcanoes. More precise time and stratigraphic frameworks have been developed using cores from swamps which preserve detailed eruption records that can be interrogated for both eruption frequency and petrologic changes (Turner et al., 2008; 2009). While these techniques have enabled detailed stratigraphic records to be interpreted from the medial to distal ring plain deposits for NZ volcanoes, the remaining challenge is to correlate these ash dominated stratigraphies to the proximal, lava-dominated sequences of the volcanic edifices. While some progress can be made with on-edifice stratigraphy (Gamble et al., 2003; Price, et al 2012), detailed cone to ring plain correlation remains elusive.

Notwithstanding the cone to ring plain correlation challenge, the data from both edifice and ring plain deposits does allow construction of 4-D models of volcano architecture (3-D and time) that can be used to interpret volcano geology in both younger and older volcanoes.

References

Alloway B., McComb P., Neall V., Vucetich C., Gibb J., Sherburn S., and Stirling M. (2005). Jl Roy Soc.NZ 35 (1-2): 229-267.

Alloway B.V., Stewart R.B., Neall V.E. and Vucetich, C.G. (1992). Quat. Res. 38 (2): 170-179.

Froggatt P.C. and Lowe D.J. (1990). NZ Jl Geol. Geophys 33 (1): 89-109.

Gamble J.A., Price R.C., Smith I.E.M., McIntosh W.C. and Dunbar, N.W. (2003). Jl Volc. Geotherm. Res. 120 (3-4): 271-287.

Lowe D.J., Shane P.A.R., Alloway B.V. and Newnham, R.M. (2008). Q. Sci. Rev. Volume 27 (1-2): 95-126.

Newnham R.M., Eden D.N., Lowe D.J. and Hendy C.H. (2003). Quat. Sci Rev. 22 (2-4): 289-308.

Pillans B. (1990). New Zealand Geological Survey miscellaneous series map 18, Wellington, New Zealand. Department of Scientific and Industrial Research.

Price R.C., Gamble J.A., Smith E.M., Maas R., Waight T., Stewart R.B., and Woodhead J., (2012). Journal of Petrology 53, (10): 2139-2189.

Stewart R.B., Neall V.E., Pollok J.A. and Syers J.K. (1977). Aust. Jl Soil Res. 15: 177 - 190.

Stokes S., Lowe D.J. and Froggatt P.C. (1992). Quat. Interntl 13-14: 103-117.

Tost M., Cronin S.J., Procter J.N., Smith I.E.M., Neall, V.E. and Price R.C. (2015). Bull. Geol. Soc. Am. 127 (1-2): 266-280.

Turner M.B., Bebbington M.S., Cronin S.J. and Stewart R.B. (2009). Bulletin of Volcanology 71 (8): 903-918.

Turner M.B., Cronin S.J., Stewart R.B., Bebbington M. and Smith, I.E.M., (2008). Geology 36 (1): 31-34.

Vucetich C.G. and Pullar, W. A. (1964). Stratigraphy and Chronology of Late Quaternary Volcanic Ash in Taupo, Rotorua and Gisborne Districts (Part 2). NZ Geol. Surv. Bull. n.s. 73.

Zernack AV, Cronin SJ, Bebbington MS, Price RC, Smith IEM, Stewart RB, Procter JN (2012) Forecasting catastrophic stratovolcano collapse: A model based on Mount Taranaki, New Zealand. Geology 40(11):983-986.

Zernack AV., Procter JN., Cronin SJ. (2009) Sedimentary signatures of cyclic growth and destruction of stratovolcanoes: A case study from Mt. Taranaki, New Zealand. Sedimentary Geology 220(3-4):288-305.

Mapping volcaniclastic deposits in the Călimani-Gurghiu-Harghita Neogene volcanic range, Romania. A brief history and current challenges

Alexandru Szakács[1, 2] & Ioan Seghedi[2]

[1] Sapientia University, Dept. of Environmental Sciences, Cluj-Napoca, Romania; [2] Romanian Academy, Romanian Academy, Institute of Geodynamics, Bucharest, Romania.

One of the most challenging tasks when mapping in ancient volcanic areas is to distinguish, genetically diagnose, and assign map units to, volcaniclastic deposits. Volcaniclastic lithologies are particularly widespread and diverse in the Călimani-Gurghiu-Harghita Neogene volcanic range (CGH), East Carpathians, Romania, covering at least 50% of the volcanic areas, especially at their western low-laying peripheries. On modern (i.e. in the 60-80's last century) geological maps at various scales (1:1,000,000,1:500,000,1:200,000,1:50,000) the distinction among the areas covered by clastic rocks adopted the model of „structural compartments". The lower compartment, thought as resulting from an early, prevailingly explosive stage of volcanic activity was considered as formed through built-up, erosion and destruction of previous volcanic structures, included all volcaniclastic deposits within a general lithological unit, denominated the "volcano-sedimentary formation" (VSF), represented on maps – at scales 1:200,000 and 1:50,000 - as an unique unit all along the whole CGH. Based on their petrographic composition, only interbededd lava flows and small-sized intrusive bodies were shown as details on larger-scale maps.

In the upper ("stratovolcanic") compartment, supposed to be generated during the second stage of evolution as a consequence of mostly effusive activity, the volcaniclastic deposits were mainly considered, and represented as so, of pyroclastic origin. At the westernmost peripheries of the range some "lahar deposits" were also depicted on the maps, but they were considered very late, post-volcanic Quaternary epiclastic deposits, actually not being parts of the two-compartment model of CGH. This kind of cartographic representation of the volcaniclastic deposits was challenged in the late 1980's and in the 1990's when the "two compartment" structural model was replaced by a "facies model", based on a large number of radiometric datings indicating that volcanic rocks (both coherent and clastic) occurring in peripheral and axial parts of the range are of similar age, and age differences can only be found between volcanic edifices. However, the map representation of volcaniclastic deposits remained as challenging as before. The breakthrough was achieved by detailed investigation, and recognition of, the various genetic types of volcaniclastic rocks of different petrographic and chemical compositions belonging to particular volcanic edifices, during the 1:50,000 scale mapping program conducted by the Geological Institute of Romania. During 1990-2000 occurrence of two large-volume debris avalanche deposits (DAD's), the Rusca-Tihu DAD and the Varghis DAD, were recognized in the western part of CGH. In the these circumstances, the new series of maps started to integrate geochronological and rock-genetical data into the cartographic representation of the newly investigated areas of CGH. As a consequence, the new

maps did not fit with the old ones and compromise solutions were applied. Unfortunately, the new mapping endeavor could not be completed because the halt of the program in the 1990's. However, in some parts of the range, where the 1:50,000 scale mapping has been completed, and the new structural concept applied, such as in the Calimani Mts. and northern part of the Gurghiu Mts., self-consistent and detailed maps emerged in which volcanologically significant lithostratigraphic map units (i.e formations) were introduced, the volcanological features are well represented and easily read, and the affiliation of certain formations to particular volcanic edifices is clear. Despite this, the lithostratigraphic approach, as used and applied now in various volcanic areas in the world (especially in Italy), is only partly implemented and integrated with the volcanic facies concept. Major difficulties in assigning map units to volcaniclastic formations arise from a number of circumstances, including 1) the tight spacing of adjoining, coevally or successively active volcanoes and interaction (interfingering, merging and superposition) of their volcaniclastic products of similar to identical composition, and 2) the occurrence of large-volume debris avalanche deposits (DAD's) transgressing facies boundaries of individual volcanic edifices or even segments of CGH, such as the Rusca-Tihu DAD originated in the Calimani Mts., but covering large areas at the periferies and beneath Gurghiu Mts. Recent discovery of another large-volume DAD originating from the Fancel-Lapusna volcano in the northern Gurghiu Mts. will further simplify map representation of volcaniclastic deposits in the western part of CGH.

Facies analysis of a Late Miocene lava dome field in the Tokaj Mts. (Carpathian-Pannonian Region): Implication for a silicic caldera structure?

J. Szepesi [1,2], S. Harangi[1], R. Lukacs[1], E. Pál-Molnár [1,2]

[1] MTA-ELTE Volcanology Research Group, Pázmány sétány 1/C, H-1117 Budapest, Hungary, szepeja@gmail.com, (szabolcs.harangi@geology.elte.hu); [2] Department of Mineralogy, Geochemistry and Petrology, University of Szeged, H-6722, Szeged Egyetem u. 2, Hungary, (palm@geo.u-szeged.hu).

Subaerial silicic effusive volcanism commonly form high viscosity, thick (up to 100 m), short (less than a few kilometres), small- to medium volume (< 1 km3) lava flows and domes. Their emplacements are often connected to silicic calderas, although they could form also lava dome fields. The Miocene (from ca. 15 Ma to 10 Ma) volcanic activity of the Tokaj-Slanske Mountains in the northeast segment of the Pannonian Basin was characterized by intense silicic volcanism in addition to eruption of andesitic magmas. The subsequent tectonic events and erosion exposed uniquely the inner structure of the rhyolitic lava domes enabling the reconstruction of their evolution. A comparison of the palaeovolcanic features with those of the characteristics of young lava domes provide a challenging way to understand better the emplacement mechanism of silicic effusive products and also to conduct the volcano geology methodology in a palaeovolcanic area.

The Telkibánya Lava Dome Field (TLDF) was formed in the northern part of the Tokaj Mts. at around 13 Ma (Fig. 1). It extends over 30 km2 and the volcanic formations have a maximum thickness of over 300 m. The spatial distribution of the eroded silicic extrusions and the covering andesite flows (Fig.1) shows strong structural alignment which is controlled by the regional NW-SE (and perpendicular) striking fault system in accordance to the stress field of Late Miocene regional extension. We performed a detailed field work accompanied with petrologic and geochemical study in order to map the lava dome structures. As a result, we concluded that the extrusive event could have occurred after a major explosive event. The pyroclastic series conformably deposited on shallow marine sediments, however, developments of the lava domes were taken place in subaerial environment at least in two phases.

Lithofacies associations

The surface outcrops and the revised borehole database offer a good opportunity to obtain detailed records of silicic lava dome/flow stratigraphy. The substantial textural heterogeneity and zonation were interpreted as a result of changing temperature (cooling rate), mechanical stress, and vesiculation processes within the subaerial cooling lava bodies. The mapped lithofacies units can be subdivided into five main lithofacies associations based on their specific textural-structural features developed during their emplacements: volcaniclastic deposits, coherent rhyolite, rhyolite-perlite transition zone, coherent glass (perlite) and fragmented carapace.

Volcaniclastic deposits: The silicic lavas extruded on extended pyroclastic deposits (up to 50m). The typical massive lapilli tuffs (mLT) are followed by stratified (sLT) and usually reversely graded,

lithoclast-rich pumiceous, perlitic lapilli tuff (mlLT) units. In addition, we could recognize clast-supported lithic breccia layers (mlBr).

Coherent rhyolite

The coherent rhyolite (CR) is the most common lithofacies within the TLDF units. The groundmass is usually devitrified in variable scales and involves high temperature crystallization domains (HTCDs) in macro (lithophysae, spherulite) and micro scale (axiolith, felsite). Based on the inner structure of the CR, three sub-facies zones can be distinguished: massive, flow-banded and vesicular subunits.

Rhyolite-glass (perlite) transition zone

A transition between the crystallized and glassy lava dome parts was developed in variable thicknesses (m-10m's). Based on the textural characteristics perlitic rhyolite (usually devitrified) and rhyolitic perlite zones were distinguished. The transition occurs in two main types: a, alternation of decimetre thick rhyolite and perlite bands in a usually strongly foliated texture, b, lithophysae and "megaspherulites" (up to 50 cm in diameter, Fig.2) in perlite. The lithophysae show more-or-less equidimensional or slightly elongated shape with coalescence in the direction of flow layering. Cavities are filled with by vapour phase crystallization products as tridymite and opal varieties.

Coherent perlite

The coherent glass (now perlite) unit is subdivided into two subzones: the inner, mostly vesicle free, typical perlite and the marginal vesiculated, pumiceous lithofacies. This pumiceous perlite usually grades into clast-rotated breccias of the fragmented carapace. The thickness of this lithofacies is in the range from a few metres up to 40 metres. The common banding is by typical fluidal texture and/or vesicle elongation. The colour of the hydrated glass is vary from black (obsidian-like perlite) to grey (typical perlite) as a result of H2O diffusion rate. The porosity ratio of pumiceous perlite ranges from 60 % (like common pumice) to 5% toward the perlite zone.

Fragmented carapace

The monolithological, matrix-poor (<20%), clast-supported breccias contain mainly subangular to very well rounded pumiceous perlite. Red and black coloured breccias are embedded between the pumiceous perlite breccia and coherent perlite zone and include fragments (mm-cm sized) of both lithology units. This facies has a lenticular shape with a sharp upper contact towards the covering breccia and grading down to the coherent glass.

Interpretation of the TLDF volcano stratigraphy

a. Within the TLDF succession lava dominated dome/flow complexes and surrounding pyroclastic apron are distinguished. They were formed during major explosive volcanic events followed by intense lava dome extrusion activity and epithermal mineralization.
b. A large negative gravity anomaly (-24 mGal) was recognized under the TLDF in a sharp contrast of local maxima (-7 mGal) of subvolcanic intrusion and low sulphidation type alteration area (Fig.1).

c. Occurrence of the silicic lithofacies units and the geophysical data suggest an approximately 20 km wide caldera formed by collapse event after the initial explosive volcanism. The subsequent post-caldera resurgence was characterized by lava dome activity.
d. The massive lapilli tuffs are interpreted as typical ignimbrites with gas segregation pipes and charcoal, whereas the bedded, well-sorted lithofacies has a pyroclastic fall origin. The reversely graded perlitic lapilli and block-rich facies could have probably derived from lava dome-related pyroclastic density currents.
e. Erosion exposed all the main lithological units of an idealized lava dome-flow complex at different levels. The thickness/surface ratio varied in the function of the erosion rate. The coherent rhyolite zones are interpreted as the core facies of eroded lava domes and flows. The textural heterogeneity of transition zone reflects variations in cooling rate with development of HTCDs (lithophysae and spherulite). The “megaspherulites” described here are rare worldwide. The coherent glass developed by enhanced cooling and later underwent strong devitrification. The pumiceous perlite could represent the finely vesicular pumice units of recent lava domes. The fragmented carapace in a complex architecture surrounds the coherent lava flow/dome units. The clast distribution refers to mechanical disruption during extrusion. The texture of red and black breccias implies secondary vesiculation event releasing volatile phases.
f. The present day morphology reflects the preservation potential of the lithological units rather than the original depositional geometry. The erosional volume (8.5 km3) are quite similar to other moderate to large volume lavas (Mono-Inyo Chain-California, Badlands Rhyolite-Idaho,) The estimated volume of the silicic lavas could have been certainly more than 10 km3.

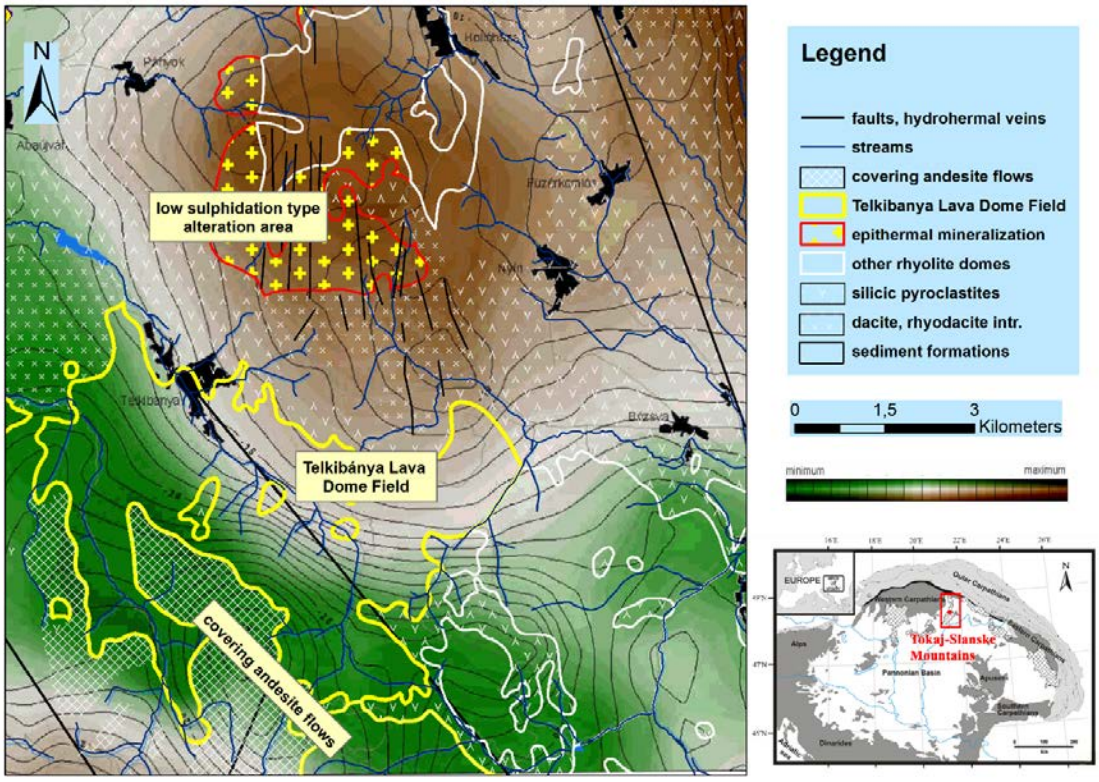

Fig. 1 - *Gravity Bouguer-anomaly map of Kiss and Zelenka (2009) with the geological-volcanological interpretation of Telkibánya Lava Dome Field. Colours from calculation by □=2.0 g/cm3, isolines from □=2.67 g/cm3. Reference: Telkibánya Geology Publ. Univ. Miskolc, Series A, Mining 78, 97-115.*

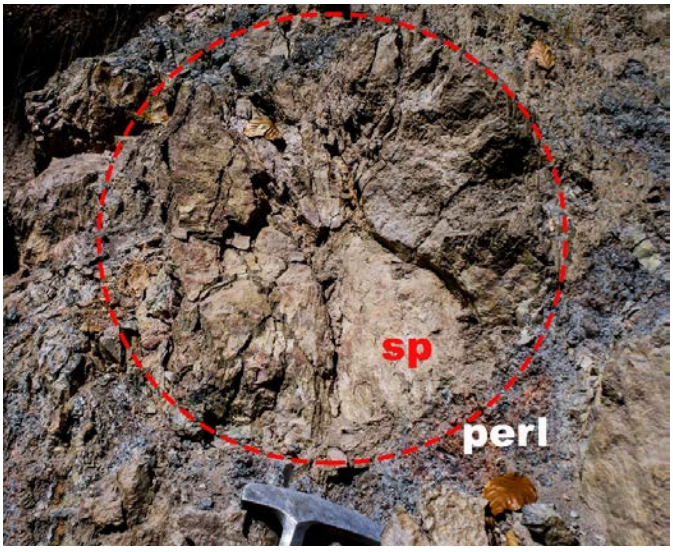

Fig. 2 - *The largest high temperature crystallization domain "megaspherulite" 0.5 m <) with radial jointing in perlite from perlite–rhyolite transition at the base of Cser Hill dome.*

Mapping and fieldwork in ancient volcano sites – an example from the Lausitz Volcanic Field (Eastern Germany)

Olaf Tietz, Jörg Büchner & Erik Wenger

Senckenberg Museum of Natural History Görlitz (olaf.tietz@senckenberg.de).

1. The Lausitz Volcanic Field – the modern knowledge, an overview. The Lausitz Volcanic Field (LVF) is part of the Central European Volcanic Province (CEVP). It covered manly the uplifted Lausitz Block, a Cadomian-Variscan consolidated block-faulted area and the northern margin of the North Bohemian Cretaceous Basin (Fig. 1). The age of the volcanic rocks ranges from about 35 to 26 Ma. Volcanism was associated with tectonic movements and Cenozoic lignite basin development. In the LVF roughly 500 vents (volcanic centers) are exposed in more than a thousand volcanic outcrops (Büchner et al., 2015). In general the volcanic rocks in the LVF represent an alkaline trend typical for intra-continental suites. The volcanism is dominated by nephelinite/basanites and phonolithe/trachytes. This bimodal distribution is reflected by the volcanology and morphology of the volcanic remnants. Scoria cones are the most frequent type at the LVF. These are relatively small basaltic volcanoes, of which only the hard "core" is preserved, represented by the lava lake fillings, feeder dykes, plugs or lava flows. Phonolithic and trachytic rocks formed mostly small monogenetic domes or cryptodomes. The edifices of the volcanoes are mostly denudated, and the pyroclastic rocks are predominantly missing. Only the lava bodies are partly preserved with conspicuous hills in the landscape (Fig. 2).

2. Methods of ancient volcano mapping – fieldwork to day. Intensive field observation, connected with a detailed geological mapping of some selected volcano sites provided to a new volcanological view and interpretation for the Lausitz Volcanoes since 2010 (see references). These investigations could found at some localities remnants of pyroclastic rocks, such as volcanic scoriae, tuffs or diatreme breccias. The pyroclastic rocks play a key role for the reconstruction of the volcanic eruption style and the former volcano type. Therefore, only a detailed mapping could yield this imported documents. But large areas of the rock surface of Central Europe are cover by soil and vegetation or urbane structures. Only about 5 - 10 % of the volcano areas in the LVF build up rock cliffs or cutting slopes, such as from ways, rivers or temporary pits. Therefore a geological documentation of the volcano sites is only possible by profile grit mapping in combination with the collecting of bedrock fragments, in some cases by little excavation holes and test bores. This field documents must be additional connected with the digital elevation model (DEM) in a high resolution (up to 2 m grit), because the mapping units could better bounded by morphological features, such as slope gradients or hill shapes.

3. Examples of volcano sites – results of detailed research. Three Cenozoic volcano remnants (Baruth, Landeskrone, Sonnenberg) were investigated in the Lausitz Volcano Field in detail for a

physical-volcanological reconstruction of the former volcano edifices.The Baruth Complex Volcano consists of three deeply eroded scoria cones with remnants of nephelinitic and basanitic lavas. Only in glaciofluviatile Saalian-1-Glaciation sediments and in a sheltered position appear greater amounts of scoria pebbles. They proof the scoria cone volcano type. Additionally geophysical, petrographical and geochemical investigations and isotopic age determination supported the subdivision in three single volcanoes, which penetrate each other at nearly the same locality (Tietz et al. 2011a). The Landeskrone Volcano is a large monogenetic scoria cone with an imposing conical hill about 110 m over the granodioritic basement. Today we find mainly the lava lake filling as dense nephelinite. The developed columnar jointing with a dip direction almost inclined outward the present hill allow in connection with a small remnant of scoria cone at the hill foot the reconstruction of the lava lake and the eroded scoria cone. This volcano reconstruction shows a deepening and widening of the scoria cone by a presumably phreatomagmatic eruption before the final lava lake filling (Tietz and Büchner 2012). The Sonnenberg Volcano is situated in Zittau Mountains 1.3 km southward the Lausitz Block in a tectonical uplifted position 200 m over the Lausitz Block. The eroded small monogenetic scoria cone volcano is poorly exposed, only a small tephritic cliff and some bedrock-fragments exist. A 10 x 10 m grit of flat excavations holes allows the mapping of the 200 x 250 m structure with diatreme breccias (uplifted northern margin), brown and red scoriae (central, with a brown rim and e red centre) and a marginal lava flow. The lava lake was broken out through the crater wall to south, because of the inclination of the pre-volcanic paleosurface (Tietz et al., 2011b).

4. The aim – a reconstruction of volcanic and postvolcanic history in time and space. The three selected examples show, that intensive field work in connection with additionally investigations (use of DEM, petrography/geochemistry, age determination) allows a reconstruction of simply and complex monogenetic volcano structures with an age from about 30 Ma. Furthermore, the precise data base allows a reconstruction of the landscape evolution since the volcanic time, because the volcanoes protect and mark the synvolcanic landsurface (Tietz and Büchner 2015). The aim will be a 3D modeling of the uplift and denudation history of the area, when some more volcanoes sites are mapped and reconstructed.

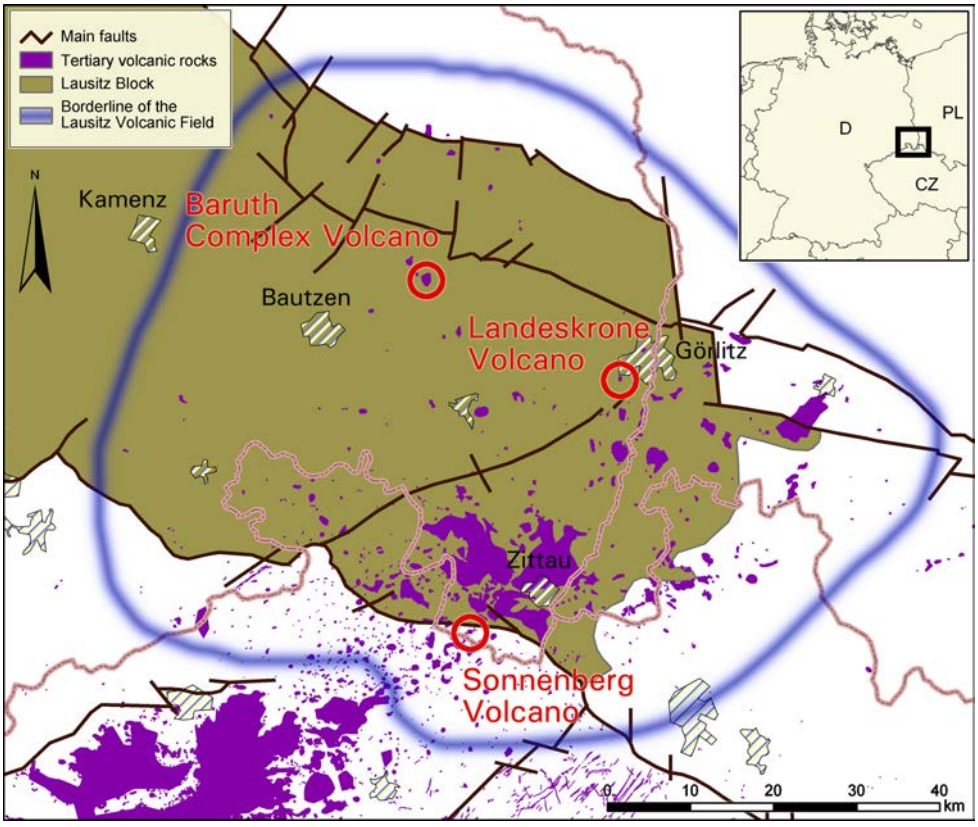

Fig. 1 - *Map of the LVF with the descript volcano sites.*

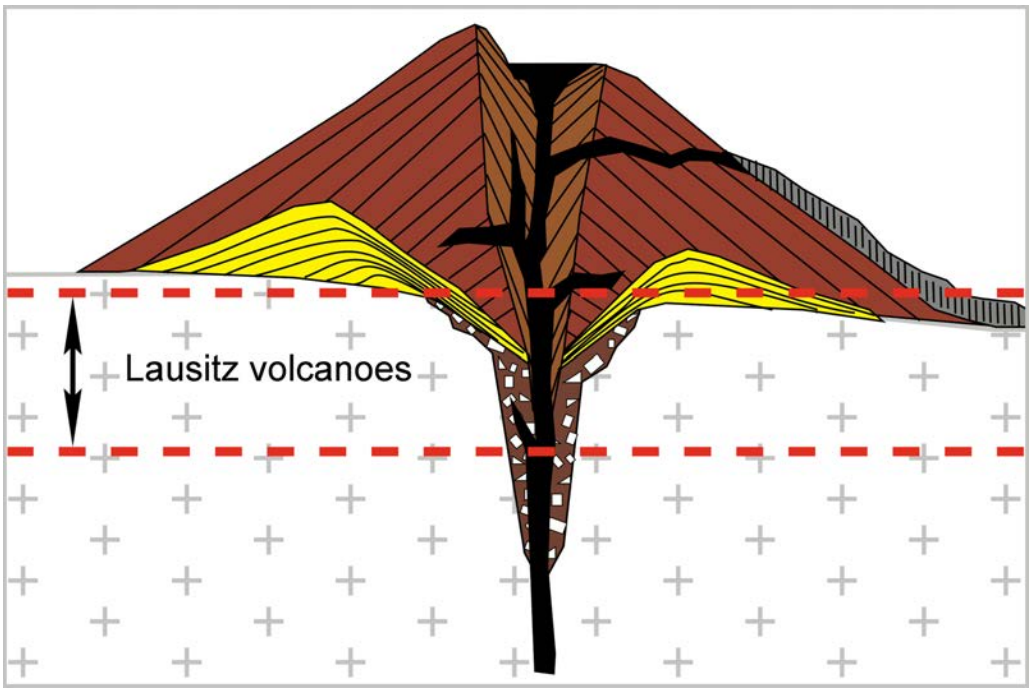

Fig. 2 - *Usual range of erosion level for the volcanoes in the LVF.*

References

Büchner J. and Tietz O. (2012). Reconstruction of the Landeskrone Scoria Cone in the Lusatian Volcanic Field, Eastern Germany: Insights on a large sized monogenetic volcano, long-lasting degradation of volcanic edifices and implications for the landscape evolution. Geomorphology, 151–152, 175–187.

Büchner J., Tietz O., Viereck L., Suhr P. Abratis,M. and P. van den Bogaard (2015). Volcanology, Geochemistry and Age of the Lausitz Volcanic Field: International Journal of Earth Sciences, 104, 2057–2083.

Tietz O., Büchner J., Suhr P., Abratis M. and Goth K. (2011a). Die Geologie des Baruther Schafberges und der Dubrauker Horken. Aufbau und Entwicklung eines känozoischen Vulkankomplexes in Ostsachsen. Berichte der Naturforschenden Gesellschaft der Oberlausitz, Supplement zu Band 18, 15–48.

Tietz O., Gärtner A.and Büchner J. (2011b). The monogenetic Sonnenberg scoria cone: implications for volcanic development and landscape evolution in the Zittauer Gebirge Mountains since the Paleogene. Zeitschrift für Geologische Wissenschaften 39, 5/6, 311–334.

Tietz, O. and Büchner J. (2015). The landscape evolution of the Lausitz Block since the Paleozoic with special emphasis to the neovolcanic edifices in the Lausitz Volcanic Field (Eastern Germany). Zeitschrift der Deutschen Gesellschaft für Geowissenschaften / German Journal of Geosience 166, 2, 125–147.

Geology and evolution of Volcanic Complex Yucamane-Calientes (Tacna-Perù)

Jessica Vela[1], Marco Rivera[1], Pablo Samaniego[2]

[1]Volcano Observatory of INGEMMET (Directorate of Environmental Geology and Risk). Carolina_20v@hotmail.com
[2] Laboratoire Magmas et Volcans, Université Blaise Pascal, CNRS, IRD.

The Yucamane-Calientes volcanic complex consists of two stratovolcanoes. The Yucamane volcano (5,550 meters above sea level-msnm) is located in the south of this complex and the volcano Calientes (5980 m) is located in the north of this complex. The Yucamane is the most recent and active volcano, it was formed in the upper Pleistocene-Holocene. The complex Yucamane-Calientes belongs to the Central Volcanic Zone of the Andes (CVZ), according to Francis Thorpe (1979). The Yucamane volcano has a cone shape, the difference in elevation between the base and the summit is 1200 m, and it has an area of approximately 20 km^2. This volcano is composed of a succession of lavas, covered by reworked ash. At the top there are two craters, the larger crater is 900 m of diameter and the smaller crater is 400 m of diameter and 200 m of depth. The other volcano, the Calientes volcano is partially destroyed. The only part of the volcano that is still intact is the western end of the volcano and within this volcano there is a dome called "Calientes Dome".Based on geological, stratigraphic, radiometric dating (40K/40Ar, ^{14}C) and our interpretation of satellite images Landsat TM and ASTER, we believe the following steps happened in the next chrono- stratigraphic evolution: The Calientes volcano was built on the remnants of an ancient volcano (Yucamane Chico) after an important ignimbrite sequence (ignimbrite "Calientes"), dated at 540 ka (France, 1985). The Calientes volcano has three developmental stages: "Calientes I, II and III", during which andesitic and dacitic lavas are mainly emplaced which happened as a result of effusive activity. After this the Yucamane volcano was formed in three consecutive periods: "Yucamane I", was emplaced by andesite lava and basic andesite flows. In the second stage "Yucamane II", less than 36 ka emplaced collapses of domes associated with dome complex. Finally in the third stage "Yucamane III" emplaced andesitic and dacitic lavas flows, which now form the upper cone of the volcano. The activity of the young cone Yucamane was characterized by a recurring explosive activity responsible for generating pyroclastic flows and escoria falls with low volume (<0.01 km^3), and a pumice fall deposit product of a subpliniana eruption, which occurred 3270 years ago. The present study was performed to determine the Yucamane past eruptive behavior of the volcano, as well as the threats and risks that involve reactivation for prevention and mitigation. The assessment of volcanic hazards associated with Yucamane is crucial especially in the foot of the southern flank of the volcano because at least six villages are located near the souther flank: Candarave, Cairani, Huanuara, Quilahuani, Susapaya, Ticaco, among others, where there are more than 8,000 inhabitants (INEI, 2008).

Mapping volcanic areas: broad Eruption unit criteria vs UBUs. The case of Hellenic South Aegean volcanic centers

Georges E. Vougioukalakis

Institute of Geology and Mineral Exploration, Athens Greece,(gvoug@igme.gr).

South Aegean volcanic edifices had been mapped since 1981, mostly aiming to the volcanic hazard assessment of the area, and we always used the typical approach of “eruption” units criteria in a broader sense. This define a unit to be mapped as a single large explosive eruptive event, or a period of mainly effusive – extrusive – mild explosive activity fed by magmas of similar petrographic – petrologic characteristics, defining practically a body in the contest of a lithostratigraphic unit, a formation of the geological map. This resulted very useful not only to assess volcanic hazard and estimate relative risk, but to any kind of needed information for exploration, exploitation and land use of these areas. Trying to apply USUs criteria in volcanic areas, we faced serious problems, mostly because the criteria to define, e.g. if an epiclastic deposit represent a “significant” episode in time and space to be taken into consideration, are not still used with an objective and accurate method in volcanic terrains.

On the other hand, using the “eruption’ unit method, we had communication and understanding problems with stratigraphers while we were working in the Aegean area. Aiming to discuss these ideas and problems, we present three 1:10,000 scale geological maps of the South Aegean volcanic edifices: Kimolos island (Late Pliocene – Early Quaternary age), Nisyros island (160-~20 ky BP) and Thirasia island (Santorini island group, 172-3.6 ky BP), to use them as base for discussion and exchange of ideas.

Lava flow morphology as a proxy for lava flow rheology: mapping rheological transitions in basaltic lava flows

Alan Whittington[1], Arianna Soldati[1], Alexander Sehlke[1,2], Benedicte Robert[3], Etienne Médard[3], Andrew Harris[3], Lucia Gurioli[3], Gustavo Chigna[4]

[1]Department of Geological Sciences, University of Missouri, Columbia MO 65203 USA, (whittingtona@missouri.edu / sol); [2] NASA; [3] Clermont-Ferrand; [4] INSIVUMEH, Guatemala City, Guatemala.

Lava morphology, on coarse and fine scales, reflects the rheological behavior of the flow during emplacement. Rheological behavior of lava is in turn controlled by temperature, composition, crystal content, bubble content, and strain rate. We have estimated rheological properties such as viscosity and yield strength from the dimensions of lava flows at Kilauea and Pacaya, and characterized the surface morphology on the pahoehoe to `a`a spectrum. These observations are compared with experimental viscosity measurements by concentric cylinder viscometry, to quantify the conditions of the pahoehoe-`a`a transition. The Muliwai a Pele lava channel was emplaced during the final stage of Mauna Ulu's 1969–1974 eruption (Kilauea, Hawaii). The event was fountain-fed and lasted for around 50 h, during which time a channelized flow system developed, in which a 6-km channel fed a zone of dispersed flow that extended a further 2.6 km. All thermal and rheological parameters (cooling, crystallization rate, viscosity, and yield strength) experienced a change around 4.5 km from the vent. At this point, there is a lava surface transition from pahoehoe to `a`a. Lava density, microlite content, viscosity, and yield strength all increase down channel, but vesicle content and lava temperature decrease. Cooling rates derived from MgO thermometry were ~6.7˚C/km, with crystallization rates increasing from 0.03 Φc/km proximally, to 0.14 Φc/km distally, where Φc is the crystal volume fraction. We quantified the viscosity-strain-rate dependence of this lava during cooling and crystallization, using concentric cylinder viscometry. We measured the viscosity of the crystal-free liquid between 1600 and 1230 °C, where we observed a deviation from the expected viscosity trend, marking the liquidus. We then made rheology measurements at subliquidus temperatures of 1207, 1203, 1183, 1176, and 1169 °C, varying the applied strain rates at each temperature. While the crystal-free liquid behaved as a Newtonian fluid, crystallization changed the rheological response to pseudoplastic behavior, even at the lowest crystal volume fraction of 0.025. Pseudo-plastic behavior was observed down to a temperature of 1183 °C, with a crystal fraction of 0.15. Between 1183 and 1176 °C, the two-phase suspension transitioned from a power-law fluid to a Herschel-Bulkley fluid. At temperatures of 1176 and 1169 °C, with crystal fractions of 0.33 and 0.42, respectively, we observed lobate surface textures on the experimental samples, which remained preserved until the end of the experiments. Measurements at these temperatures indicated yield strengths of 82±16 and 238±18 Pa, respectively.

The yield strength resulted from the development of an interconnected crystal network of diopside and enstatite by 1176 °C. By 1169 °C, diopside and plagioclase microcrystals had also appeared, and the effective viscosity was between 2000 and 5000 Pa s, depending on the strain rate. Further cooling to 1164 °C resulted in a rapid viscosity increase, to an effective viscosity in excess of 105 Pa s that exceeded the measurement range of our apparatus. The yield strength varies with crystallinity in an exponential fashion, with yield strength in Pa given by σy=1.25e12.93Φc. In our experiments, the transition from pahoehoe to `a`a occurred between 1200 and 1170 °C, at viscosities between 100 and 1000 Pa s, depending on strain rate. We also mapped, sampled, and recorded video of the 2014 flow on the southern flank of Pacaya, Guatemala. Velocimetry data extracted from videos allowed us to determine that lava traveled at ~2.8 m/s on the steep ~45˚ slope 50 m from the vent, while 550 m further downflow it was moving at only ~0.3 m/s on a ~4˚ slope. Estimates of effective viscosity based on Jeffreys' equation increased from ~7,600 Pa s near the vent to ~28,000 Pa s downflow. In the laboratory we measured the viscosity of a representative lava composition using a concentric cylinder viscometer, at 5 different temperatures between 1234˚C and 1199˚C, with crystallinity increasing from 0.1 vol% to 40 vol%. The rheological data were best fit by power law equations, with the flow index decreasing as crystal fraction increased, and no detectable yield strength. Although field-based estimates are based on lava characterized by a lower temperature, higher crystal and bubble fraction, and with a more complex petrographic texture, field estimates and laboratory measurements are mutually consistent and both indicate shear-thinning behavior. The complementary field and laboratory data sets allowed us to isolate the effects of different factors in determining the rheological evolution of the 2014 Pacaya flows. We assess the contributions of cooling, crystallization, and changing ground slope to the 3.7-fold increase in effective viscosity observed in the field over 550 m, and conclude that decreasing slope is the single most important factor over that distance. It follows that the complex relations between slope, flow velocity, and non-Newtonian lava rheology need to be incorporated into models of lava flow emplacement.

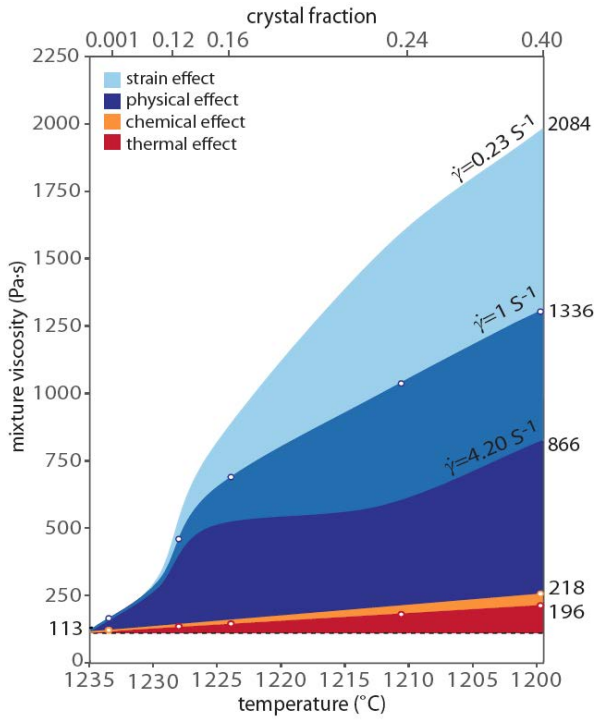

Fig. 1 - *Measured apparent viscosity of 2014 Pacaya lavas as a function of temperature and crystallinity. Remelt composition is shown in red, evolved composition in orange, and two-phase (melt + crystals) mixture in different shades of blue, for three different strain rates (0.23, 1, and 4.2 s-1) which correspond to the highest and lowest observed while the flows were active.*

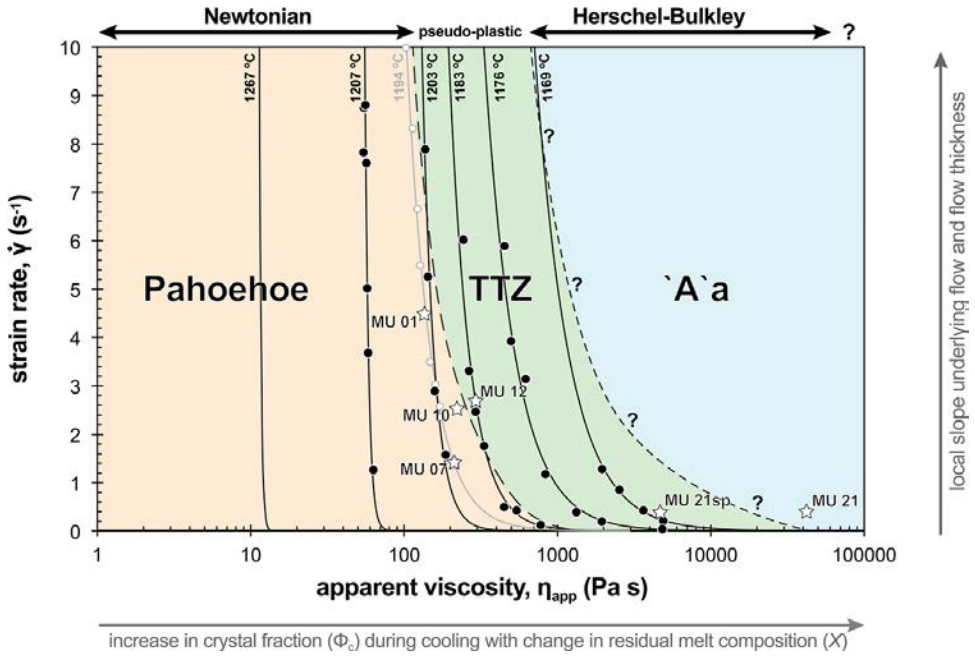

Fig. 2 - *Experimental measurements of apparent viscosity (black dots) against strain rate for lavas from Mauna Ulu, fitted by power-law flow curves (Sehlke et al. 2014). Stars indicate observed flow surface morphology (Robert et al. 2014).*

References

Robert B., Harris A.J.L., Gurioli L., Médard E., Sehlke A.*, and Whittington, A., (2014). Textural and rheological evolution of basalt flowing down a lava channel. Bulletin of Volcanology, 76: 824, doi: 10.1007/s00445-014-0824-8

Sehlke A.*, Whittington A.G., Robert B., Harris A.J.L., Gurioli L., and Médard E., (2014). Pahoehoe to `a`a transition of Hawaiian lavas: an experimental study. Bulletin of Volcanology, 76: 876, doi: 10.1007/s00445-014-0876-9.

Soldati A.*, Sehlke A.*, Chigna G., and Whittington A.G., (2016). Field and experimental constraints on the rheology of arc basaltic lavas: the January 2014 Eruption of Pacaya (Guatemala). Bulletin of Volcanology, in press.

Pyroclastic fall simulation with TEPHRA2 for FOR Puracè Volcano (COLOMBIA) from historical eruptions data

Indira Zuluaga-Mazo[1], Maria L. Monsalve[1], John J. Galarza[2]

[1]Colombian Geological Survey - SGC, izuluaga@gov.co; [2]Colombian Geological Survey - SGC- Volcanological and Seismological Observatory of Popayán.

Puracé volcano (2˚18'23.56''N; 76˚22'50.14''; 4630 asl) is located in the Central Cordillera of Colombian Andes, as part of the volcanic Chain Los Coconucos, 27 km from Popayan, capital of Cauca Department, SW of Colombia. (Fig.1). The Puracé volcano considered one of the most active volcanoes in Colombia, has been permanent monitored by Volcanological and Seismological Observatory of Popayán (Colombian Geological Survey); field and geological research is carried out to update its volcanic hazard map, using among others, simulation tools for volcanic phenomena based on its geological record, which includes deposits of: pyroclastic density currents, lavas, lahars, ballistic eject and pyroclastic falls. The deposits of these falls, correspond to those left by the historical activity, and are limited to the highest areas of the volcano (Fig. 2), while fall deposits associated to older eruptions are meager or nonexistent. The software "Tephra2" (Bonadonna et al., 2014) from the research group VHUB (Collaborative volcano research and risk mitigation) was used (on line) to simulate future scenarios of pyroclastic falls from Puracé Volcano. Considering the scarcity of field data needed for the inputs of this computational tool, the required parameters were determined from interpretation and analysis of historical information, and field data obtained in the higher areas of the volcano. Based on these data, isopachs were drawn and areas of dispersion were postulated (Fig. 3), also using laboratory techniques, the density of representative deposits was determined and the eruptive mass was calculated.

The historical documents analyzed were descriptions of explorers and scientists that visited the volcano and its activity, newspapers releases, and stories transmitted orally, which provided information on height and spread of eruptive columns, thickness and grain size of the material erupted in several episodes that occurred between 1849 and 1977, activity that is named "Historical Eruptive Unit of Purace volcano" (Monsalve el at, 2012). Based on these interpretations, the results of simulations generated isovalues mass maps of material and prevailing directions of dispersion (Fig. 4), from which scenarios of pyroclastic falls are formulated, as an essential component for volcanic hazard assessment of Puracé volcano. This work was done in the framework of Colombian Geological Survey research project for elaboration and updating of volcanic hazard maps for active volcanoes in Colombia, in cooperation with Vhub.

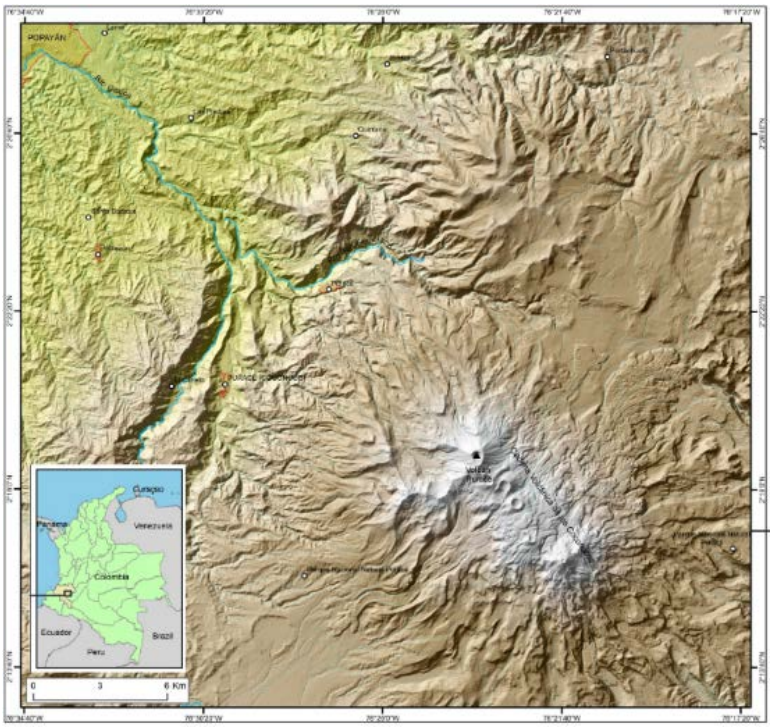

Fig. 1 - *Puracé Volcano localization.*

Fig. 2 - *Fall deposits left by the historical activity.*

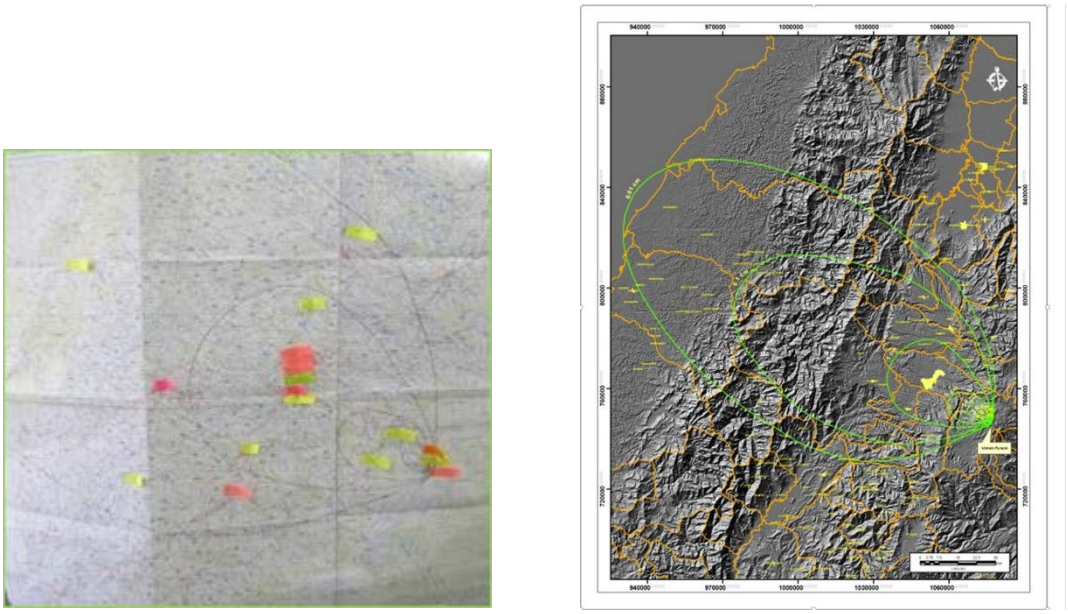

Fig. 3 - *Reconstruction of isopachs from analysis and interpretation of historical documents.*

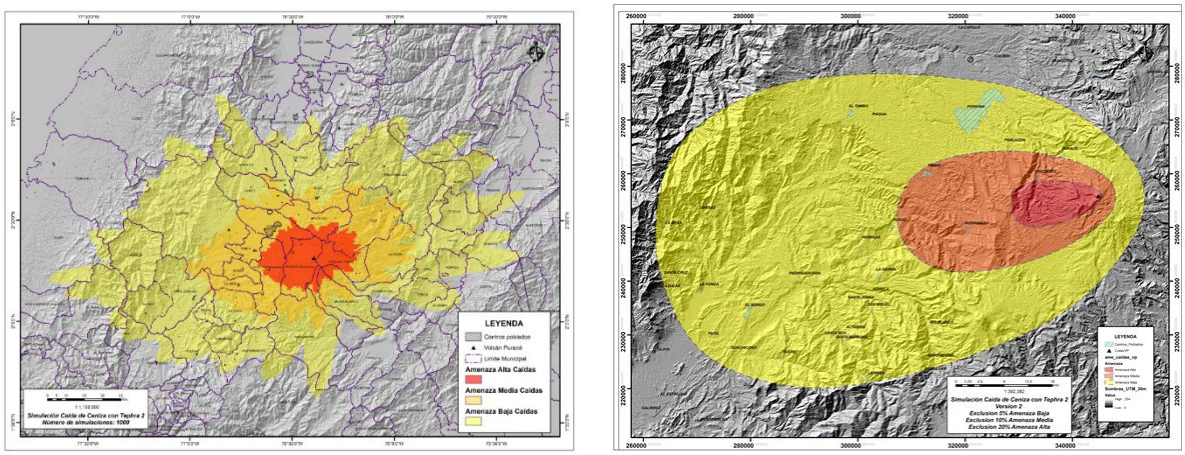

Fig. 4 - *Results of simulations with Tephra2, for pyroclastic falls of Puracé Volcano.*